

Cells^{Q1} of Extraembryonic Mesodermal Origin Confer Human Dystrophin in the Mdx Model of Duchenne Muscular Dystrophy

YAYOI KAWAMICHI,^{1,2,3} CHANG-HAO CUI,¹ MASASHI TOYODA,¹ HATSUNE MAKINO,¹ AKANE HORIE,¹ YORIKO TAKAHASHI,¹ KENJI MATSUMOTO,⁴ HIROHISA SAITO,⁴ HIROAKI OHTA,² KAYOKO SAITO,³ AND AKIHIRO UMEZAWA^{1*}

¹Department of Reproductive Biology, National Institute for Child Health and Development, Tokyo, Japan

²Department of Obstetrics and Gynecology, Tokyo Women's Medical University, Tokyo, Japan

³Institute of Medical Genetics, Tokyo Women's Medical University, Tokyo, Japan

⁴Department of Allergy and Immunology, National Institute for Child Health and Development, Tokyo, Japan

Duchenne muscular dystrophy is an X-linked recessive genetic disease characterized by severe skeletal muscular degeneration. The placenta is considered to be a promising candidate cell source for cellular therapeutics because it contains a large number of cells and heterogeneous cell populations with myogenic potentials. We analyzed the myogenic potential of cells obtained from six parts of the placenta, that is, umbilical cord, amniotic epithelium, amniotic mesoderm, chorionic plate, villous chorion, and decidua basalis. In vitro cells derived from amniotic mesoderm, chorionic plate, and villous chorion efficiently transdifferentiate into myotubes. In addition, in vivo implantation of placenta-derived cells into dystrophic muscles of immunodeficient mdx mice restored sarcolemmal expression of human dystrophin. Differential contribution to myogenesis in this study may be attributed to placental portion-dependent default cell state. Molecular taxonomic characterization of placenta-derived maternal and fetal cells in vitro will help determine the feasibility of cell-based therapy.

J. Cell. Physiol. 9999: 1–9, 2010. © 2010 Wiley-Liss, Inc.

The human placenta is a large discoid organ with a diameter of around 20 cm and a weight of approximately 500 g. It contains a large number of cells possessing a wide range of phenotypes and potentials (Cunningham and Williams, 2005; Sadler and Langman, 2006). The functions of the placenta are (a) exchange of metabolic and gaseous products between maternal and fetal bloodstreams and (b) production of hormones, such as progesterone, estradiol, estrogen, and human chorionic gonadotrophin. The placenta consists of the following two components: (a) a fetal portion, derived from the amnion, the chorionic plate (CP), the smooth chorion (chorion laeve (SC)), and the villous chorion (chorion frondosum (VC)) and (b) a maternal portion, derived from the decidua basalis (DB). The amnion, the inner layer, consists of a small amount of connective tissue (amniotic mesoderm (AM)) covered with a cuboidal epithelium (amniotic epithelium (AE)). The amniogenesis is rather complicated, the AM being extraembryonic whereas the AE is from the inner cell mass/embryoblast. The chorion, the outer layer of the amnion, is classified into VC, SC, and CP. The embryonic and abembryonic portions are called villous and SC, respectively. The VC is made of growing and expanding villi, while the CP and SC are made of degenerated villi. The DB, originating from the endometrium, is composed of glandular epithelial cells and stromal (mesenchymal) cells with decidual change. The umbilical cord (UC) that attaches a fetus to the placenta develops from the body stalk of the embryo and contains blood vessels and Wharton jelly, surrounded by the amnion. Each part of the placenta has recently been a candidate cell source for cell-based therapies because of the variety of cell types that become available (Fukuchi et al., 2004; Portmann-Lanz et al., 2006).

One currently untreatable disease which may benefit from cell-based therapy using placenta-derived cells is Duchenne muscular dystrophy (DMD). DMD is an X-linked recessive genetic disease characterized by severe skeletal muscle degeneration. It is caused by a deficiency in dystrophin that is associated with a large oligomeric complex of glycoproteins which provide linkage to the extracellular membrane (Ervasti and Campbell, 1991). The absence of dystrophin results in destabilization of the extracellular membrane–sarcolemma–cytoskeleton architecture, making muscle fibers susceptible to contraction-associated mechanical stress and degeneration. In the first phase of the disease, new muscle fibers are formed by

Yayoi Kawamichi, Chang-Hao Cui, and Masashi Toyoda contributed equally to this work.

Additional Supporting Information may be found in the online version of this article.

Contract grant sponsor: Ministry of Health, Labour and Welfare (Nervous and Mental Disorders);

Contract grant number: 19A-71

Contract grant sponsor: Japan Health Sciences Foundation;

Contract grant number: KHD10261

*Correspondence to: Akihiro Umezawa, National Institute for Child Health and Development, 2-10-1, Okura, Setagaya, Tokyo 157-8535, Japan. E-mail: umezawa@1985.jukuin.keio.ac.jp

Received 25 August 2009; Accepted 22 December 2009

Published online in Wiley InterScience
(www.interscience.wiley.com.), 00 Month 2010.
DOI: 10.1002/jcp.22076

satellite cells. After depletion of the satellite cell pool in childhood, skeletal muscles degenerate progressively and irreversibly and are replaced by fibrotic tissue (Cossu and Mavilio, 2000). No effective therapeutic approaches for muscular dystrophy currently exist; thus, cell-based therapy, in addition to gene therapy (Harper et al., 2002), exon skipping therapy (Matsuo et al., 1991), and read-through therapy by aminoglycoside (Barton-Davis et al., 1999) remain promising treatment options.

Myoblasts represent the natural first choice in cellular therapeutics for skeletal muscle because of their intrinsic myogenic commitment (Grounds et al., 2002). However, myoblasts recovered from muscular biopsies are poorly expandable *in vitro* and rapidly undergo senescence (Cossu and Mavilio, 2000). Intramuscular allotransplantation of normal muscle precursor cells can induce expression of donor-derived dystrophin in skeletal muscles of patients with DMD (Skuk et al., 2006). However, it is difficult to perform transplantation of muscle precursor cells due to a limited number of donor cells. An alternative source of muscle progenitor cells is therefore desirable. Cells with a myogenic potential are present in many tissues, including bone marrow (Ferrari et al., 1998; Dezawa et al., 2005), UC blood (Gang et al., 2004), adipose tissue (Rodriguez et al., 2005; Di Rocco et al., 2006), and endometrium and menstrual blood (Cui et al., 2007), and all these cells readily form skeletal muscle *in culture*.

There has, as yet, been no systematic analysis of the distribution of placenta-derived stem cells which have myogenic differentiation potential. Therefore, we characterized each placenta-derived cell *in vitro*, via a taxonomic approach using global gene expression profiles, and investigated which part of the placenta is the most useful source of stem cells with a myogenic potential that might prove useful for possible future cell-based therapy of DMD.

Materials and Methods

Isolation of human placental tissues

Ethical approval for tissue collection was granted by the Institutional Review Board of the National Institute for Child Health and Development, Japan. Written informed consent was obtained before the sample collection. Human placental samples were collected from normal full-term pregnancies. All of the placentas were processed within 24 h of collection and washed extensively with phosphate-buffered saline (PBS). After peeling off the amnion, the placenta was separated into three parts, that is, CP, VC, and DB. To isolate cells from the UC, the middle part was used, after excluding the edge of the placenta and the tissue close to the fetal navel. The amnion and the SC were manually separated. Amniotic mesodermal cells were manually scraped from the AE. After each placental part was minced using scissors, minced AM was re-suspended in MSCGM (Cambrex Bio Science, Walkersville, MD). We did not calculate the cell numbers at the start of cultivation because the tissue was chopped up mechanically by hand. The placenta-derived cells were maintained at 37°C in a humidified atmosphere containing 5% CO₂ and allowed to attach for 48 h. Non-adherent cells were removed and the medium was changed twice a week. At 70–80% confluence, the cells were harvested with trypsin (0.25%) and 1 mM EDTA (0.02%) in PBS (1:1, v/v) and plated to new dishes. Primary culture cells were used, except for the differentiation analysis. Cells were processed from 45 placentas, and primary cultures from 10 placentas were used for this study.

Flow cytometric analysis

Flow cytometric analysis was performed as previously described (Terai et al., 2005). Briefly, cells were incubated with primary antibodies or isotype-matched control antibodies, followed by

additional treatment with the immunofluorescent secondary antibodies. Cells were analyzed on an EPICS ALTRA analyzer (Beckman Coulter, Fullerton, CA). Antibodies against human CD13, CD14, CD29, CD34, CD44, CD45, CD55, CD59, CD73, CD90, CD105, CD166, HLA-ABC, and HLA-DR were purchased from Beckman Coulter, Immunotech (Marseille, France), Cytotech (Hellebaek, Denmark), and BD Biosciences Pharmingen (San Diego, CA).

In vitro myogenesis

In vitro myogenic analysis was performed as previously described (Cui et al., 2007). Briefly, placenta-derived cells were seeded onto 60-mm collagen I-coated cell culture dishes (BD Biocoat™) at a density of 1×10^5 /ml in growth medium (Dulbecco's modified Eagle's medium (DMEM), supplemented with 20% fetal bovine serum (FBS)). Forty-eight hours after seeding onto collagen I-coated dishes, the cells were treated with 5 μM 5-azacytidine for 24 h. Cell cultures were then maintained in differentiation medium (DMEM, supplemented with 2% horse serum). The differentiation medium was changed twice a week until the experiment was terminated.

Reverse transcriptase-polymerase chain reaction analysis (RT-PCR) of placenta-derived cells

RT-PCR analysis was performed as previously described (Cui et al., 2007). Briefly, RT-PCR of MyoD, Myf5, myogenin, myosin heavy chain-11x/d (MyHC-11x/d), desmin, and dystrophin was performed with 2 μg of total RNA. The sequences of PCR primers that amplify human but not mouse genes are listed in Supplementary Table 1. PCR was performed for 30 cycles, with each cycle consisting of 94°C for 30 sec, 60°C or 65°C for 30 sec, and 72°C for 20 sec, with additional 10-min incubation at 72°C after completion of the last cycle.

Fusion assay in vitro

Placenta-derived cells ($2,500/\text{cm}^2$) were co-cultured with C2C12 myoblasts ($2,500/\text{cm}^2$) for 2 days in DMEM supplemented with 10% FBS, and then cultured for seven additional days in DMEM with 2% horse serum to promote myotube formation. C2C12 myoblast cells were supplied by RIKEN Cell Bank (The Institute of Physical and Chemical Research, Japan). The cultures were fixed in 4% paraformaldehyde (PFA) and stained with a mouse anti-human nuclei IgG1 monoclonal antibody (clone 235-1, Millipore[®]) and a mouse anti-myosin heavy chain IgG2b monoclonal antibody (MF-20, Developmental Studies Hybridoma Bank, University of Iowa, IA). The cells were visualized with appropriate Alexa-fluor-conjugated goat anti-mouse IgG1 and IgG2b secondary antibodies (Molecular Probes, Eugene, OR). Total cell nuclei were stained with 4', 6-diamidino-2-phenylindole (DAPI). To assess the ability of placenta-derived cells to fuse with C2C12 cells, we calculated the percentage of myotubes containing one or more human nuclei in the total myotube as a fusion index.

In vivo cell implantation

The cells (2×10^7) were suspended in PBS, in a total volume of 100 μl, and directly injected into the right tibialis anterior muscle of 6- to 8-week-old mdx/mdx scid/scid (mdx-scid) mice. The mice were euthanized 4 weeks after cell implantation, and the right tibialis anterior muscle was analyzed for human dystrophin by immunohistochemistry.

Immunohistochemical and immunocytochemical analysis

Immunohistochemical and immunocytochemical analyses were performed as previously described (Mori et al., 2005). Briefly, the sections were incubated with a mouse anti-human dystrophin IgG2a monoclonal antibody (NCL-DYS3, Novocastra, UK), and then incubated with horseradish peroxidase-conjugated rabbit anti-mouse immunoglobulin. Staining was developed using a

solution containing diaminobenzidine and H_2O_2 . Slides were counterstained with hematoxylin. In the cases of fluorescence, frozen sections fixed with 4% PFA were used. The anti-human dystrophin monoclonal antibody, anti-human nuclei mouse monoclonal antibody, anti- α -sarcoglycan rabbit IgG polyclonal antibody (H-82, Santa Cruz Biotechnology⁰³) or anti-laminin 2 α rat IgG monoclonal antibody (4H8-2, Sigma-Aldrich⁰⁴) was used as the initial antibody, and goat anti-mouse IgG2a conjugated with Alexa Fluor 546, goat anti-mouse IgG1 antibody conjugated with Alexa Fluor 488, goat anti-rabbit IgG conjugated with Alexa Fluor 635, or goat anti-rat IgG conjugated with Alexa Fluor 488 was used as a second antibody. The anti-myogenin mouse monoclonal antibody (F5D, BD Pharmingen⁰⁵) was used for immunocytochemistry. As a methodological control, the primary antibody was omitted. In the cases of fluorescence, the slides were incubated with Alexa Fluor 546-conjugated goat anti-mouse IgG antibody.

GeneChip expression analysis

Human genome-wide gene expression was examined with the Human Genome U133 Plus 2.0 Array (GeneChip; Affymetrix, Inc., Santa Clara, CA), which contains the oligonucleotide probe set for more than 47,000 transcripts and variants, including approximately 40,000 well-characterized human genes and expressed sequence tags (ESTs). Total RNA was prepared from samples using the RNeasy Kit (Qiagen⁰⁶), according to the manufacturer's instructions. The purity of RNA was assessed on the Agilent Bioanalyser 2100. Double-stranded cDNA was synthesized from DNase-treated total RNA, and the cDNA was subjected to *in vitro* transcription in the presence of biotinylated nucleoside triphosphates using the Enzo BioArray HighYield RNA Transcript Labeling Kit (Enzo Life Sciences, Inc., Farmingdale, NY) according to the manufacturer's protocol. The biotinylated cRNA was hybridized with a probe array for 16 h at 45°C, and the hybridized biotinylated cRNA was stained with streptavidin-PE (query 6) and scanned with a Hewlett-Packard Gene Array Scanner (Palo Alto, CA). The fluorescence intensity of each probe was quantified using the GeneChip Analysis Suite 5.0 computer program (Affymetrix) and Robust Multi-array Average (RMA) model (Bolstad et al., 2003; Irizarry et al., 2003a,b). To normalize the variations in staining intensity among chips, the "average difference" values for all genes on a given chip were divided by the median value for expression of all genes on the chip. To eliminate genes containing only a background signal, genes were selected only if the raw values of the "average difference" were more than 200, and if the expression of the gene was judged to be "present" by the GeneChip Operating Software version 1.4 (Affymetrix).

Hierarchical clustering and principal component analysis (PCA)

The hierarchical clustering and PCA techniques classify data by similarity of expression pattern using NIA Array Analysis and TIGR Mev (<http://lgsun.grc.nia.nih.gov/ANOVA/>, <http://www.tm4.org/mev.html>).

Results

Morphology of placenta-derived cells

We collected 45 normal full-term placentas which were then separated into six parts, that is, UC, AE, AM, CP, VC, and DB (Fig. 1). Ten placentas were used for the subsequent experiments. Primary cells from each separated part were successfully cultured. These cultured cells appeared to be two morphologically different groups: small fibroblast-like cells and epithelium-like cells (Fig. 2Aa–g). Cells derived from the UC, AM, CP, VC, and DB showed fibroblast-like morphology. However, AE-derived cells and some DB-derived cells exhibited a small cobblestone-like morphology. We obtained 1×10^6 cells after 3-week cultivation of 1 cm^3 of UC, AM, CP,

and VC; and 1×10^6 cells after 4-week cultivation of 1 cm^3 of AE and DB.

Surface marker expression and gene chip analysis

Surface markers of primary culture placenta-derived cells, in the absence of any inductive stimuli, were evaluated by flow cytometric analysis (Fig. 2B, Supplementary Figs. 1–5). The cells in "early" primary culture (with low replication number) exhibited a heterogeneous pattern by flow cytometric analysis as shown in Supplementary Figure 5. The "CP" shows two peaks (61.1% positive and 38.9% negative) for CD29 (Supplementary Fig. 5A), and the "DB" contains cells negative for CD29 (8.0%) (Supplementary Fig. 5B). In contrast, the cells in "late" primary culture (with high replication number) show a homogenous pattern by flow cytometric analysis due to the culture conditions in which mesenchymal cells can predominantly proliferate. UC-, AE-, AM-, CP-, VC-, and DB-derived cells were positive for CD13, CD29, CD44, CD55, CD59, CD73, CD90, CD105, and CD166. Placenta-derived cells expressed neither hematopoietic lineage markers, such as CD34, nor monocyte-macrophage antigens, such as CD14 (a marker for macrophage and dendritic cells), or CD45 (leukocyte common antigen). The lack of expression of CD14, CD34, or CD45 suggests that all cells cultured in our experimental setting are depleted of hematopoietic cells. The cell population was positive for HLA-ABC, but not for HLA-DR. Among the placenta-derived cells, that is, UC-, AM-, AE-, CP-, VC-, and DB-derived cells, no significant difference was observed in the expression of mesenchymal stem cell markers, suggesting that the cells are of mesenchymal origin or stromal origin.

To clarify the specific gene expression profile of cells derived from each portion of the placenta, we compared the expression levels using Affymetrix GeneChip oligonucleotide arrays. RNAs were isolated from primary cultured cells of the placenta. The gene expression profile reported in this article has been deposited in the gene Expression Omnibus (GEO) database (<http://www.ncbi.nlm.gov/geo>; accession no. GSM289889-289894). We performed PCA to determine whether it is possible to discriminate cells of one part from cells of other parts in two-dimensional expression space. PCA, using all probes and 1,087 probes which were annotated with the "transcription factor," revealed that the DB-derived cells are categorized into a distinct group. Statistical analysis revealed that the DB-derived cells significantly express genes for *FOX L2*, *HOP*, *HOX D10*, *HOX D11*, and *HOX A5*. We thus analyzed the *HOX* genes by hierarchical clustering and PCA, since the cells are well categorized, especially based on the *HOX* gene family, and identified three clusters (Fig. 2C,D). Determination of cell specification via gene chip analysis revealed that the each placental cell has a distinct expression pattern of the *HOX* gene family: (a) AE- and AM-derived cells preferentially express the *HOX B* genes, such as *HOX B2*, *B6*, *B7*, and *B8*; (b) DB-derived cells express the *HOX D* genes, such as *D3*, *D4*, *D8*, *D9*, *D10*, and *D11*; (c) the others express the *HOX A* genes, *HOX A13* and *A3*.

In vitro induction of myogenic differentiation

Each distinct part of the placenta has recently been viewed as a candidate source of material for cell-based therapies. We examined, both *in vitro* and *in vivo*, whether the placenta-derived cells have a myogenic potential. Of the 54,675 genes represented on the GeneChip, skeletal muscle-specific genes such as the phospholamban, myozenin, dystrobrevin, and myosin heavy chain were expressed in cells derived from VC and the CP. Expression of these muscle-specific genes in these cells led us to hypothesize that these cells are capable of differentiating into myocytes. To prove this, cells from each part of the placenta were exposed to 5-azacytidine for 24 h and then

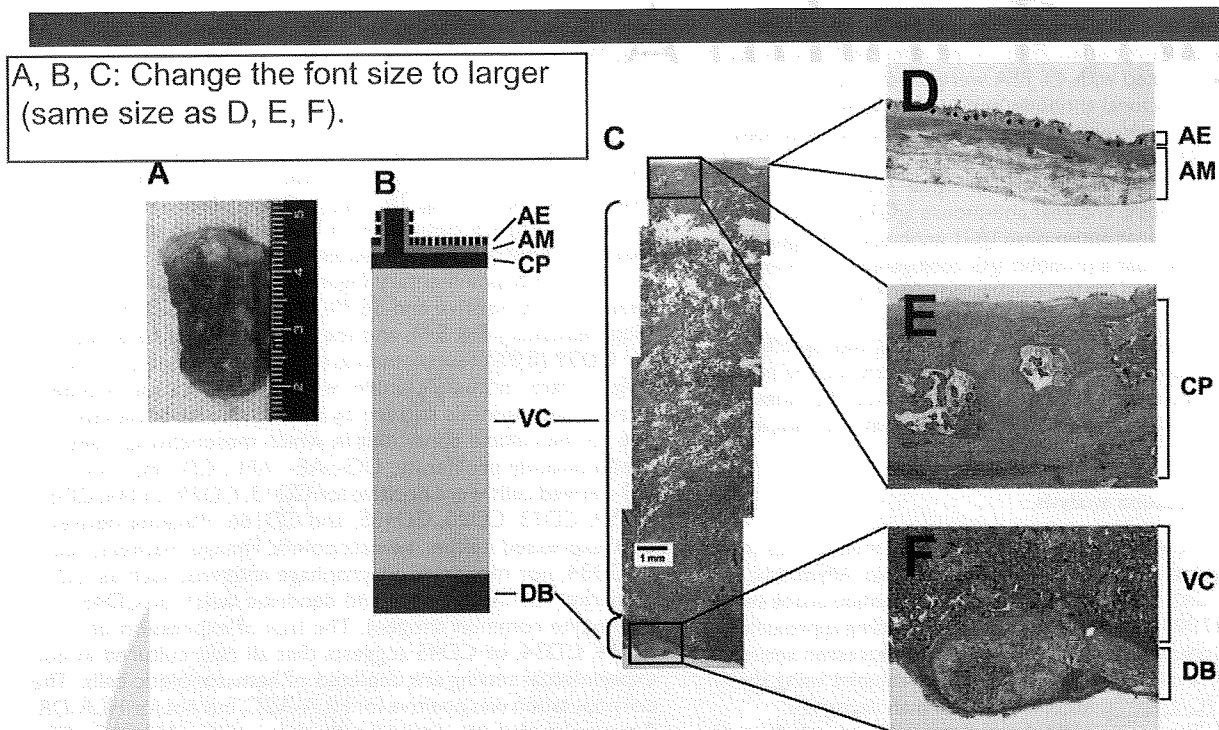


Fig. 1. Placenta-derived cells from each portion. Macroscopy (A) and histology (B,C) of amnion (D), chorionic plate (E), villous chorion, and decidua basalis (F). AE, amniotic epithelium; AM, amniotic mesoderm; CP, chorionic plate; VC, villous chorion; DB, decidua basalis.

cultured in DMEM supplemented with 2% horse serum for 3 weeks. Myogenic differentiation of the cells was analyzed by evaluating the expression of MyoD, Myf5, myogenin, MyHC-IIx/d, and desmin by RT-PCR and immunocytochemistry (Fig. 3). MyoD is constitutively expressed in amniotic mesodermal cells but decreased to no measurable level at day 3 and thereafter (Fig. 3A). In the case of the CP and VC, MyoD expression is detected at 3 weeks. Expression of genes encoding MyoD, Myf5, myogenin, and MyHC-IIx/d was under a detectable level in cells derived from UC, AE, and DB even after myogenic induction. MyHC-IIx/d, a structural gene, started to be expressed at the middle of differentiation in amniotic mesodermal cells and at the late stage in CP-derived cells. Desmin was expressed in cells derived from AM, UC, CP, AE, and DB throughout differentiation. In the cells derived from AM and CP, dystrophin expression increased after myogenic induction (Fig. 3B). Immunocytochemical analysis revealed that CP-derived cells became positive for MyHC-IIx/d, α -sarcoglycan, and myogenin after cultivation with 2% horse serum for 21 days (Fig. 3C–E). However, without any treatment, the cells did not show myotube-like morphology (Fig. 3C). C2C12 myoblasts were used for a positive control of immunocytochemistry (Supplementary Fig. 6). Placenta-derived cells from each portion exhibit different capabilities for proliferation and myogenesis in vitro (Fig. 3F).

Detection of human placental cell contribution to myotubes in an in vitro myogenesis model

To simulate in vivo phenomena, human placental cells were co-cultured in vitro with murine C2C12 myoblasts for 2 days under proliferative conditions and then switched to differentiation conditions for an additional 7 days. Multinucleated myotubes were formed after co-culturing with C2C12 cells (Fig. 4). Myosin heavy chain and human nuclei were unequivocally identified by staining with MF20 and an antibody

to human nuclei, while the numerous mouse nuclei present in this field, as shown by DAPI staining, are negative. The frequency of fusion between placenta-derived cells and C2C12 myotube depends on the cell type: cells derived from CP and DB exhibited high frequencies of fusion, whereas cells derived from AE and UC induced low-level fusion to C2C12 myocytes. No multinucleated cells were formed without co-cultivation.

Expression of human dystrophin by cell implantation in the mdx-scid mouse

To investigate whether placenta-derived cells can generate muscle tissue in vivo, cells (2×10^7) without any treatment or induction were implanted directly into the right anterior tibialis muscles of mdx-scid mice. PBS without cells was injected into the left anterior tibialis muscle as a control. After 4 weeks, myofibers in the muscle tissues injected with amniotic mesodermal cells expressed human dystrophin and laminin (Fig. 5). Dystrophin was not detected in the muscle of mdx-scid mice without cell implantation because the antibody to dystrophin used in this study is human-specific, implying that dystrophin is transcribed from dystrophin genes of human donor cells but not from reversion of dystrophied myocytes in mdx-scid mice.

Discussion

Differential myogenic potential of cultured cells from each part of the placenta

The placenta includes cells of maternal and fetal origin. Although most placenta-derived cells are of extraembryonic origin, AE-derived cells are from the epiblast/inner cell mass of the blastocyst (Cunningham and Williams, 2005; Sadler and Langman, 2006). The aim of this study was to determine the intrinsic differentiation potential of cells from six parts of the placenta, that is, UC, AE, AM, CP, VC, and DB. The myogenic potential of cells from the AM, CP, and VC proved much greater

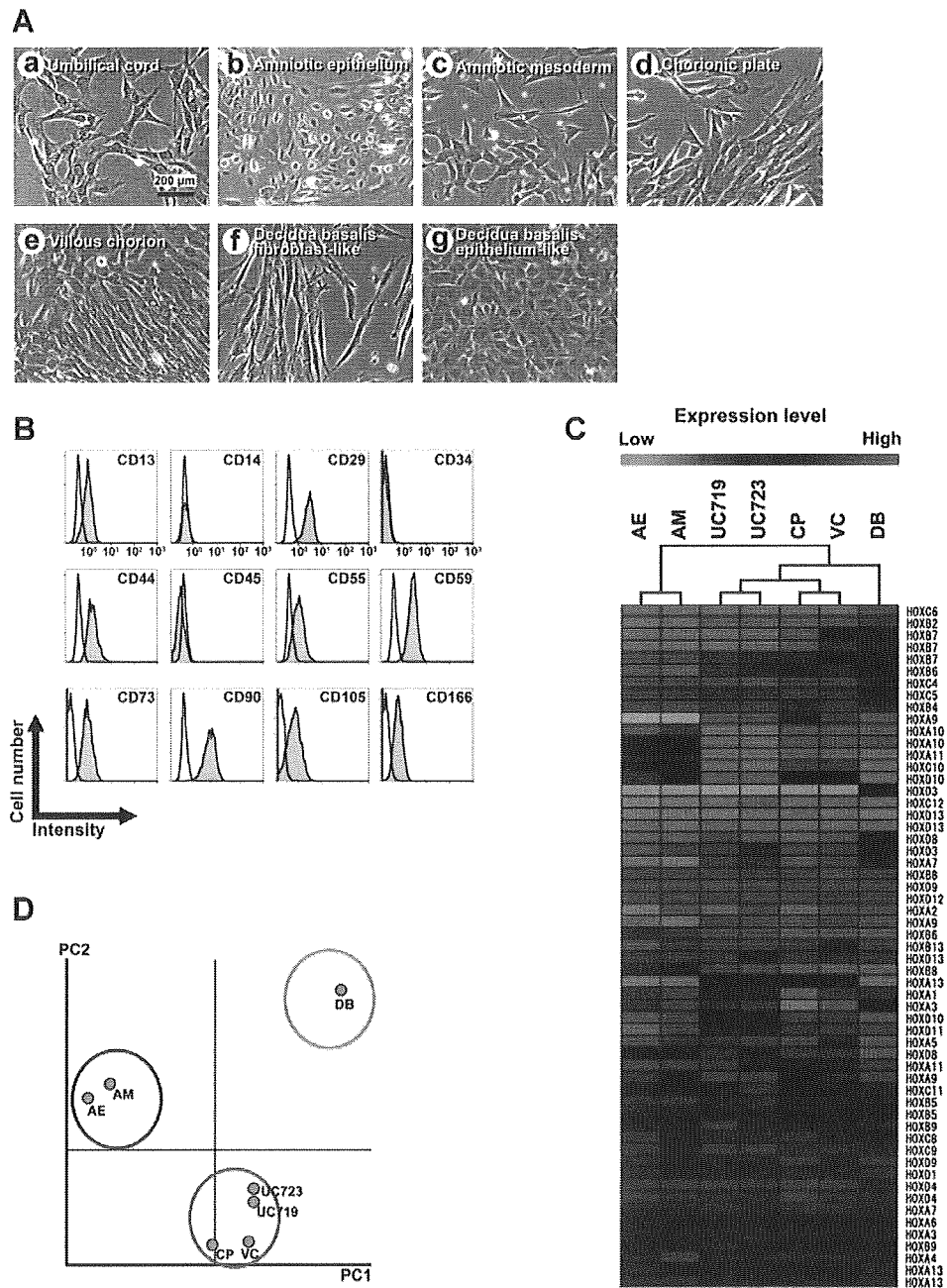


Fig. 2. Morphology of placenta-derived cells and flow cytometric analysis of amniotic mesoderm-derived cells. **A:** Photomicrographs of cells from umbilical cord-derived cells (a), amniotic epithelial cells (b), amniotic mesodermal cells (c), chorionic plate-derived cells (d), villous chorion-derived cells (e), decidua basalis-derived cells (f: fibroblast-like, g: epithelial cell-like) from primary culture. Amniotic epithelial cells (b) and decidua basalis-derived cells (g) showed an epithelial cell-like (cobblestone-like) morphology, while the others (a, c, d, e, f) showed a fibroblast-like morphology. Scale bars: 200 μ m. **B:** Flow cytometric analysis of amniotic mesoderm-derived cells in primary culture (with high replication number) in the absence of any inductive stimuli. Non-shaded and shaded areas indicated reactivity of antibodies for isotype controls and that of antibodies for cell surface markers, respectively. **C:** Hierarchical clustering analysis and heat map analysis of *HOX* gene expression in cells derived from umbilical cord (UC719 and UC723), amniotic epithelium (AE), amniotic mesoderm (AM), chorionic plate (CP), villous chorion (VC), decidua basalis (DB), using "TIGR MeV." **D:** PCA revealing general trends of *HOX* gene expression.

than expected, and this higher myogenic differentiation ratio can be a reflection of the intrinsic cellular potential of extraembryonic mesodermal cells. Lack of myogenic potential in AE-derived cells is envisaged because the cells are of extraembryonic ectodermal origin and cuboidal in morphology. Despite our findings, amniotic epithelial cells have been

reported to have the potential to differentiate to all three germ layer cells, including myocytes, after in vitro sphere formation (Miki et al., 2005). Amniotic epithelial cells formed neither spheres nor viable supernatant cells in our experimental settings, but displayed a cobblestone appearance with an epithelial phenotype. Cells obtained from AE, we believe,

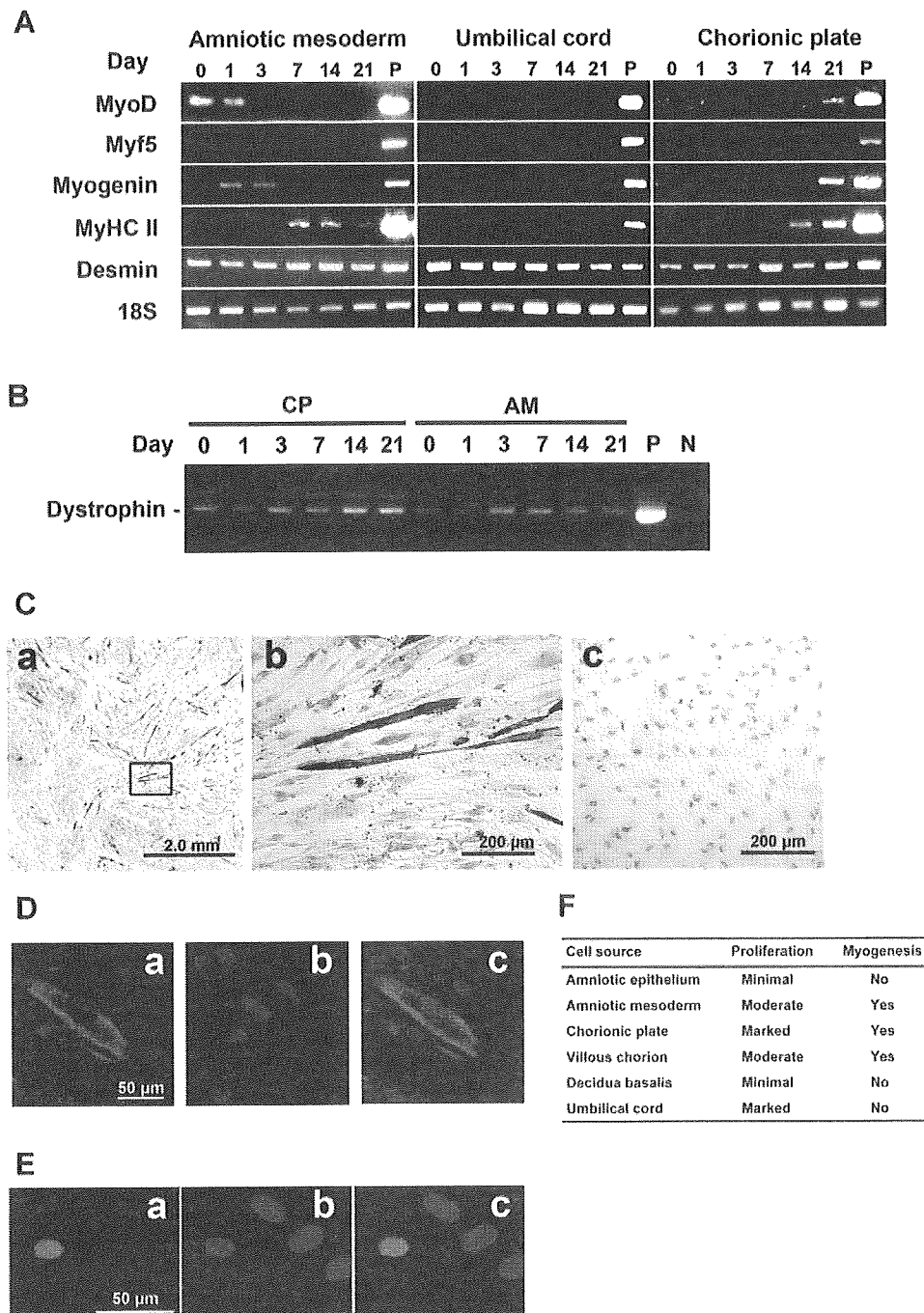


Fig. 3. Expression of muscle-specific genes during differentiation of placenta-derived cells. **A:** RT-PCR analysis of human MyoD, Myf5, myogenin, myosin heavy chain type IIx/d (MyHC-IIx/d), desmin, and 18S cDNA (from top to bottom). Umbilical-cord-derived cells, amniotic mesodermal cells, and chorionic plate-derived cells were exposed to 5 μ M 5-azacytidine for 24 h and then subsequently cultured in DMEM supplemented with 2% HS for 21 days. RNAs from human muscle serve as a positive (P) control. Only the 18S PCR primer used as a positive control reacted with the human and murine cDNA. **B:** RT-PCR analysis of human dystrophin in chorionic plate (CP) and amniotic mesodermal cells (AM). The muscle-specific isoform (Dp427m) was amplified. RNAs from human muscle serve as a positive (P) control. **C:** Immunocytochemistry of skeletal myosin heavy chain in chorionic plate-derived cells after myogenic induction (a,b) or no induction (c). Scale bars: (a) 2.0 mm, (b,c) 200 μ m. **D:** Immunocytochemistry of α -sarcoglycan. a: α -sarcoglycan; b: DAPI staining; c: "merge" of a and b. Scale bars: 50 μ m. **E:** Immunocytochemistry of myogenin. a: myogenin; b: DAPI staining; c: "merge" of a and b. Scale bars: 50 μ m. **F:** Cell site origin and capability for proliferation and myogenesis.

correspond to previously reported adherent cells with little myogenic activity (Miki et al., 2005). The poor myogenic capability of UC-derived cells was also contrary to our expectation based on prior research (Conconi et al., 2006). It

may also be due to intrinsic cell characteristics (or cell mission), and UC-derived cells embedded in Wharton's jelly may be terminally differentiated cells or highly specific cells which produce a matrix for cushioning of the cord.

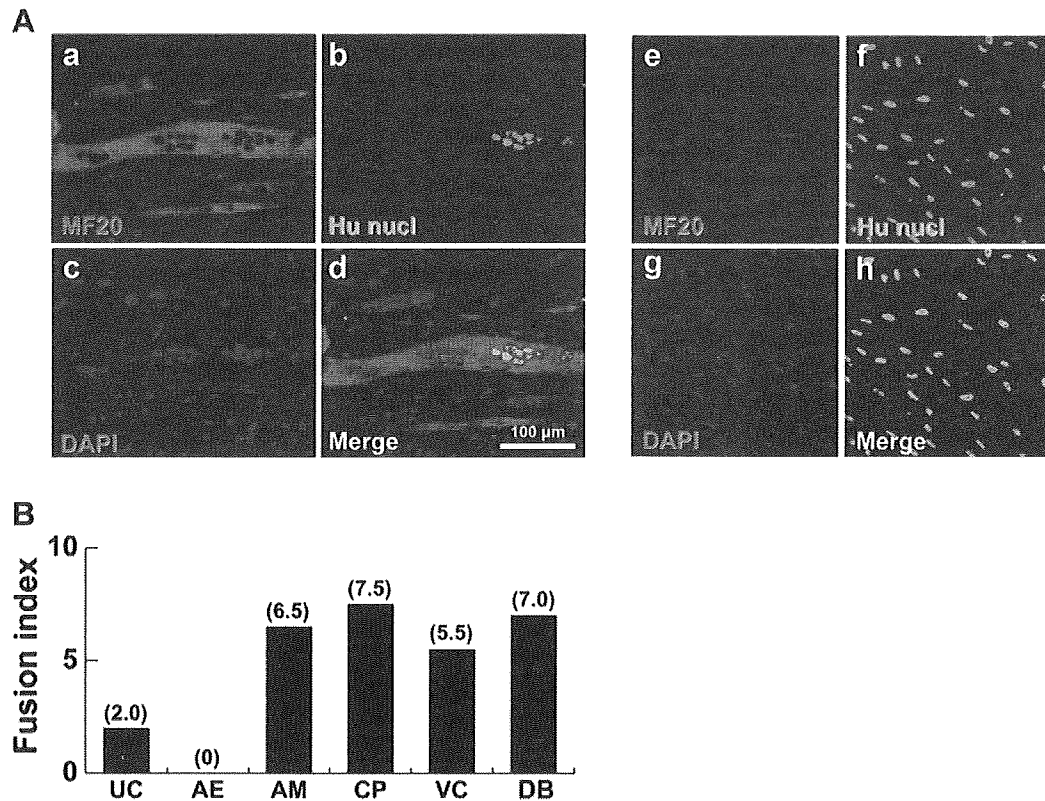


Fig. 4. Detection of human placenta-derived cell contribution to myotubes in an *in vitro* myogenesis model. The chorionic plate-derived cells were co-cultured with C2C12 myoblasts for 2 days under conditions that favored proliferation. The cultures were then changed to differentiation media for 7 days to induce myogenic fusion. **A:** Fusion between human chorionic plate-derived cells and murine C2C12 cells. **a:** human myosin heavy chain molecule (red, MF20); **b:** human nuclei (HuNucl, green); **c:** DAPI staining (blue); **d:** “merge” of **a**, **b**, and **c**. Scale bars: 100 μ m. **e-h:** Human chorionic plate-derived cells without co-culturing. **e:** human myosin heavy chain molecule (red, MF20); **f:** human nuclei (HuNucl, green); **g:** DAPI staining (blue); **h:** “merge” of **e**, **f**, and **g**. **B:** Comparison of fusion between each placenta-derived cell and mouse C2C12 myoblasts. Fusion index is shown as number of fused cells per 1,000 cells. UC, umbilical cord; AE, amniotic epithelium; AM, amniotic mesoderm; CP, chorionic plate; VC, villous chorion; DB, decidua basalis.

Taxonomic approach using global gene expression database

In general, cultured cells reflect *in vivo* characteristics, for example, hematopoietic cells proliferate as a supernatant cell in culture, and epithelial cells exhibit cobblestone appearance at confluence. In contrast, mesenchymal/stromal cells from each part of the placenta, regardless of cell source, show similar appearance *in vitro* and *in vivo*, irrespective of their diversity with respect to differentiation and proliferation. The different phenotypes of mesenchymal/stromal cells are maintained even after a series of cell replications and passages, probably by epigenetics, such as genomic methylation and chromatin of cells. The stably transmitted epigenetics in cultured cells reflects a gene expression network and maintains cell identity, and thus each mesenchymal cell is predictable by the results of gene expression with GeneChip analysis. Categorization of the cells may reflect the native functional difference, even after cultivation, and implies that cells from the UC, AE, AM, CP, VC, and DB have a distinct cell identity, in addition to mesenchymal or epithelial phenotypes.

Cell-based therapy for DMD

DMD is a fatal disease for which an effective treatment is still being actively sought. As a novel treatment option, stem cells could be used to replace defective dystrophin and restore the dystrophic muscles. Most placenta-derived cells are either

myogenic progenitors or have myogenic potential, and clearly cells with the highest myogenic potential would be beneficial for treatment of dystrophic muscle. Acquisition or recovery of dystrophin expression in dystrophic muscle is attributed to two different mechanisms: (a) myogenic differentiation of implanted or transplanted cells and (b) cell fusion of implanted or transplanted cells with host muscle cells. In this study using placenta-derived cells, our findings, namely that implantation of placenta-derived cells improved the efficiency of muscle regeneration and dystrophin delivery to dystrophic muscle in mice, are explained by both possibilities or the latter possibility (fusion mechanism) alone. Efficient fusion systems of placenta-derived cells with host dystrophic myocytes may contribute substantially to a major advance toward eventual cell-based therapies for muscle injury or chronic muscular disease.

The isolation of tissue-specific stem cells for expansion *in vitro* and transplantation back into the patient in an allogeneic manner is indeed an ideal strategy, from the viewpoint of industry-based, sustainable supply of large quantities of affordable, quality-controlled cells. In most cases of degenerative diseases and genetic diseases, such as lysosomal storage diseases, it is unlikely that enough unaffected stem cells will be isolated or available in sufficient quantity, necessitating the use of stem cells from suitable, cost-effective allogeneic sources, such as human placenta. The predicted number of AM-derived cells from one placenta of an average size (500 g)

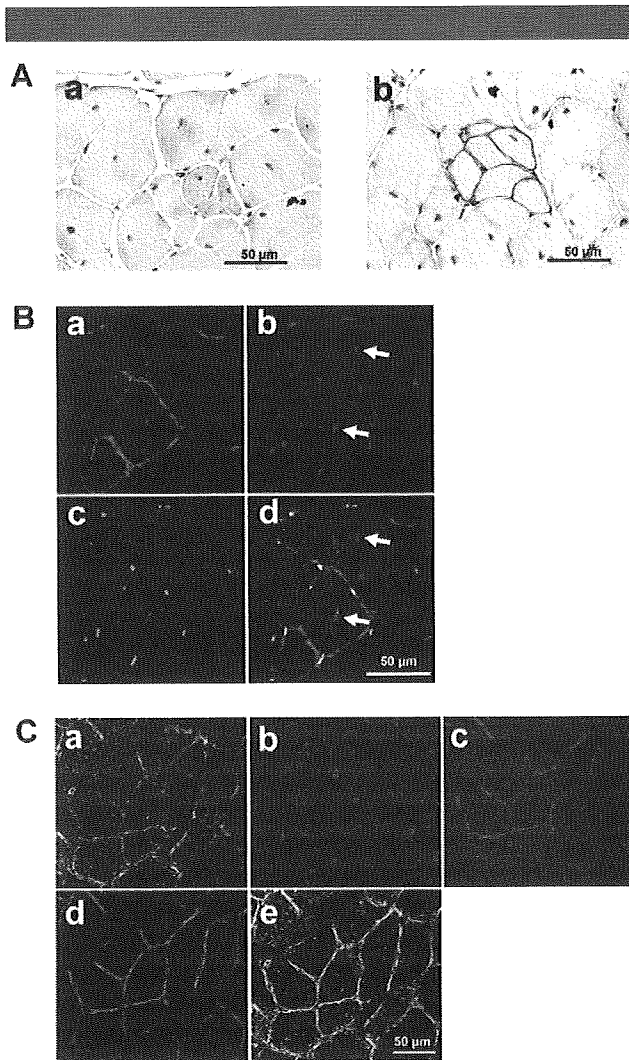


Fig. 5. Conferral of dystrophin to mdx myocytes by human placenta-derived cells. **A:** Immunohistochemistry using an antibody against human dystrophin on anterior tibialis muscle sections of mdx-scid mice after direct injection of PBS without cells (a: negative control) or amniotic mesoderm-derived cells without any treatment or induction (b) into mdx-scid myofibers. Scale bars: 50 μm . **B:** Immunohistochemistry analysis on anterior tibialis muscle sections of mdx-scid mice after direct injection of amniotic mesoderm-derived cells without any treatment or induction. Immunohistochemistry revealed the incorporation of implanted cells into newly formed myofibers, which expressed human dystrophin 4 weeks after implantation. Murine nuclei are indicated by arrows. a: human dystrophin molecule (red); b: DAPI staining (blue); c: human nuclei (HuNucl, green); d: "merge" of a, b, and c. Scale bars: 50 μm . **C:** Immunohistochemistry analysis on anterior tibialis muscle sections of mdx-scid mice after direct injection of amniotic mesoderm-derived cells. a: α -sarcoglycan (yellow); b: DAPI staining (blue); c: laminin (red); d: human dystrophin (green); e: "merge" of a, b, c, and d. Scale bars: 50 μm .

would be approximately 1×10^6 (before ex vivo amplification), possibly reaching 1×10^{11} after cultivation. This may cover 3,000 cm^3 of muscular tissues in cell-based therapy (Skuk et al., 2006). Cells converted into myotubes in vitro at a high frequency after induction, giving rise to large numbers of myofibers expressing human dystrophin when transplanted into BALB/c and mdx mice, thus fulfilling all the criteria required for a successful allogeneic cell therapy for muscular dystrophy. It should also be remembered that currently, implantation of placenta-derived cells in an allogeneic combination requires

administration of immunosuppressive drugs, such as FK506 and steroids.

We have established a method for systemic mapping of placental cells with myogenic potential. Cellular dissection and cultivation, coupled with accurate determination of the molecular characteristics of specific cells in the human placenta, opens up significant new possibilities in regenerative medicine. The outcome of this study indicates a potential cell-based treatment for DMD, a lethal human disease for which no effective treatment currently exists.

Acknowledgments

We would like to express our sincere thanks to H. Abe and M. Inoue-Yamazaki for providing expert technical assistance, to K. Saito for her secretarial work, and to A. Crump for reviewing the manuscript.

Literature Cited

- Barton-Davis ER, Cordier L, Shoturma DI, Leland SE, Sweeney HL. 1999. Aminoglycoside antibiotics restore dystrophin function to skeletal muscles of mdx mice. *J Clin Invest* 104:375–381.
- Bolstad BM, Irizarry RA, Astrand M, Speed TP. 2003. A comparison of normalization methods for high density oligonucleotide array data based on variance and bias. *Bioinformatics* 19:185–193.
- Conconi MT, Burra P, Di Liddo R, Calore C, Turetta M, Bellini S, Bo P, Nussdorfer GG, Parnigotto PP. 2006. CD105(+) cells from Wharton's jelly show in vitro and in vivo myogenic differentiative potential. *Int J Mol Med* 18:1089–1096.
- Cossu G, Mavilio F. 2000. Myogenic stem cells for the therapy of primary myopathies: Wishful thinking or therapeutic perspective? *J Clin Invest* 105:1669–1674.
- Cui CH, Uyama T, Miyado K, Terai M, Kyo S, Kiyono T, Umezawa A. 2007. Menstrual blood-derived cells confer human dystrophin expression in the murine model of Duchenne muscular dystrophy via cell fusion and myogenic transdifferentiation. *Mol Biol Cell* 18:1586–1594.
- Cunningham FG, Williams JW. 2005. Implantation, embryogenesis, and placenta development. In: *Williams obstetrics*, 22nd edition. New York: McGraw-Hill Professional, pp 39–90.
- Dezawa M, Ishikawa H, Itokazu Y, Yoshihara T, Hoshino M, Takeda S, Ide C, Nabeshima Y. 2005. Bone marrow stromal cells generate muscle cells and repair muscle degeneration. *Science* 309:314–317.
- Di Rocco G, Iachininoto MG, Tritarelli A, Straino S, Zacheo A, Germani A, Crea F, Capogrossi MC. 2006. Myogenic potential of adipose-tissue-derived cells. *J Cell Sci* 119:2945–2952.
- Ervasti JM, Campbell KP. 1991. Membrane organization of the dystrophin-glycoprotein complex. *Cell* 66:1121–1131.
- Ferrari G, Casella-De Angelis G, Coletta M, Paolucci E, Stornaiuolo A, Cossu G, Mavilio F. 1998. Muscle regeneration by bone marrow-derived myogenic progenitors. *Science* 279:1528–1530.
- Fukuchi Y, Nakajima H, Sugiyama D, Hirose I, Kitamura T, Tsuji K. 2004. Human placenta-derived cells have mesenchymal stem/progenitor cell potential. *Stem Cells* 22:649–658.
- Gang EJ, Jeong JA, Hong SH, Hwang SH, Kim SW, Yang IH, Ahn C, Han H, Kim H. 2004. Skeletal myogenic differentiation of mesenchymal stem cells isolated from human umbilical cord blood. *Stem Cells* 22:617–624.
- Grounds MD, White JD, Rosenthal N, Bogoyevitch MA. 2002. The role of stem cells in skeletal and cardiac muscle repair. *J Histochem Cytochem* 50:589–610.
- Harper SQ, Hauser MA, DelloRusso C, Duan D, Crawford RV, Phelps SF, Harper HA, Robinson AS, Engelhardt JF, Brooks SV, Chamberlain JS. 2002. Modular flexibility of dystrophin: Implications for gene therapy of Duchenne muscular dystrophy. *Nat Med* 8:253–261.
- Irizarry RA, Bolstad BM, Collin F, Cope LM, Hobbs B, Speed TP. 2003a. Summaries of Affymetrix GeneChip probe level data. *Nucleic Acids Res* 31:e15.
- Irizarry RA, Hobbs B, Collin F, Beazer-Barclay YD, Antonellis KJ, Scherf U, Speed TP. 2003b. Exploration, normalization, and summaries of high density oligonucleotide array probe level data. *Bioinformatics* 19:1494–1502.
- Matsuo M, Masumura T, Nishio H, Nakajima T, Kitoh Y, Takumi T, Koga J, Nakamura H. 1991. Exon skipping during splicing of dystrophin mRNA precursor due to an intron deletion in the dystrophin gene of Duchenne muscular dystrophy kobe. *J Clin Invest* 87:2127–2131.
- Miki T, Lehmann T, Cai H, Stolz DB, Strom SC. 2005. Stem cell characteristics of amniotic epithelial cells. *Stem Cells* 23:1549–1559.
- Mori T, Kiyono T, Imabayashi H, Takeda Y, Tsuchiya K, Miyoshi S, Makino H, Matsumoto K, Saito H, Ogawa S, Sakamoto M, Hata J, Umezawa A. 2005. Combination of hTERT and bmi-1, E6, or E7 induces prolongation of the life span of bone marrow stromal cells from an elderly donor without affecting their neurogenic potential. *Mol Cell Biol* 25:5183–5195.
- Portmann-Lanz CB, Schoeberlein A, Huber A, Sager R, Malek A, Holzgreve W, Surbek DV. 2006. Placental mesenchymal stem cells as potential autologous graft for pre- and perinatal neuroregeneration. *Am J Obstet Gynecol* 194:664–673.
- Rodriguez AM, Pisani D, Dechesne CA, Turc-Carel C, Kurzenne JY, Wdziekonski B, Villageois A, Bagnis C, Breittmayer JP, Groux H, Ailhaud G, Dani C. 2005. Transplantation of a multipotent cell population from human adipose tissue induces dystrophin expression in the immunocompetent mdx mouse. *J Exp Med* 201:1397–1405.
- Sadler TW, Langman J. 2006. Third month to birth: The fetus and placenta. In: *Langman's medical embryology*, 10th edition. Philadelphia: Lippincott Williams & Wilkins, pp 89–109.
- Skuk D, Goulet M, Roy B, Chapdelaine P, Bouchard JP, Roy R, Dugre FJ, Sylvain M, Lachance JG, Deschenes L, Senay H, Tremblay JP. 2006. Dystrophin expression in muscles of duchenne muscular dystrophy patients after high-density injections of normal myogenic cells. *J Neuropathol Exp Neurol* 155:371–386.
- Terai M, Uyama T, Sugiki T, Li XK, Umezawa A, Kiyono T. 2005. Immortalization of human fetal cells: The life span of umbilical cord blood-derived cells can be prolonged without manipulating p16INK4a/RB braking pathway. *Mol Biol Cell* 16:1491–1499.

Efficient reprogramming of human and mouse primary extra-embryonic cells to pluripotent stem cells

Shogo Nagata^{1,2}, Masashi Toyoda³, Shinpei Yamaguchi¹, Kunio Hirano¹, Hatsune Makino³, Koichiro Nishino³, Yoshitaka Miyagawa⁴, Hajime Okita⁴, Nobutaka Kiyokawa⁴, Masato Nakagawa⁵, Shinya Yamanaka⁵, Hidenori Akutsu³, Akihiro Umezawa³ and Takashi Tada^{1,2*}

¹Stem Cell Engineering, Institute for Frontier Medical Sciences, Kyoto University, 53 Kawahara-cho, Shogoin, Sakyo-ku, Kyoto 606-8507, Japan

²JST, CREST, 4-1-8 Hon-cho, Kawaguchi-shi, Saitama 332-0012, Japan

³Department of Reproductive Biology, National Research Institute for Child Health and Development, 2-10-1 Ookura, Setagaya-ku, Tokyo 157-8535, Japan

⁴Department of Developmental Biology, National Research Institute for Child Health and Development, 2-10-1 Ookura, Setagaya-ku, Tokyo 157-8535, Japan

⁵Center for iPS Cell Research and Application (CiRA), Institute for Integrated Cell-Material Sciences, Kyoto University, 53 Kawaharacho, Shogoin, Sakyo-ku, Kyoto 606-8507, Japan

Practical clinical applications for current induced pluripotent stem cell (iPSC) technologies are hindered by very low generation efficiencies. Here, we demonstrate that newborn human (h) and mouse (m) extra-embryonic amnion (AM) and yolk-sac (YS) cells, in which endogenous *KLF4/Klf4*, *c-MYC/c-Myc* and *RONIN/Ronin* are expressed, can be reprogrammed to hiPSCs and miPSCs with efficiencies for AM cells of 0.02% and 0.1%, respectively. Both hiPSC and miPSCs are indistinguishable from embryonic stem cells in colony morphology, expression of pluripotency markers, global gene expression profile, DNA methylation status of *OCT4* and *NANOG*, teratoma formation and, in the case of miPSCs, generation of germline transmissible chimeric mice. As copious amounts of human AM cells can be collected without invasion, and stored long term by conventional means without requirement for in vitro culture, they represent an ideal source for cell banking and subsequent 'on demand' generation of hiPSCs for personal regenerative and pharmaceutical applications.

Introduction

Induced pluripotent stem cells (iPSCs) have been generated through nuclear reprogramming of somatic cells via retrovirus or lentivirus-mediated transduction of exogenous reprogramming factors Oct4, Sox2, Klf4 and C-Myc (Yamanaka 2007). This has led to greatly enhanced promise for exploring the causes of, and potential cures for, many genetic diseases, as well as increased promise for regenerative medicine. Improvements in delivery methodology have further facilitated iPSC generation by minimizing the

requirement for genetic modification (Feng *et al.* 2009). Notably, generation of genetic modification-free iPSCs with reprogramming proteins (Kim *et al.* 2009; Zhou *et al.* 2009) suggests regenerative medicine with personal iPSCs could soon be realized. However, the markedly low efficiency of iPSC generation, with all adult somatic cell types tested to date, remains problematic (Wernig *et al.* 2008). Technological advancements in this field have mainly been achieved using mouse embryonic fibroblasts (MEFs), in which the efficiency of iPSC generation is 10–100 times higher than that with adult somatic cells (Yu *et al.* 2007; Wernig *et al.* 2008). Therefore, current methods would appear to be less than ideal for generating iPSCs from adult somatic cells.

Communicated by: Fuyuki Ishikawa

*Correspondence: ttada@frontier.kyoto-u.ac.jp

DOI: 10.1111/j.1365-2443.2009.01356.x

© 2009 The Authors

Journal compilation © 2009 by the Molecular Biology Society of Japan/Blackwell Publishing Ltd.

Genes to Cells (2009) 14, 1395–1404 **1395**

Here, to find nuclear reprogramming-sensitive cells collectable with no risk by physical invasion, we generated iPSCs from human and mouse newborn extra-embryonic membranes, amnion (AM) and yolk sac (YS), which consist huge amounts of discarded cells after birth. Interestingly, the efficiency of mouse iPSC (miPSC) generation from the AM was comparable to that of MEFs by retroviral transduction with *Oct4*, *Sox2*, *Klf4* and *c-Myc*. Importantly, human iPSC (hiPSC) is also efficiently generated from human AM cells. Expression of the endogenous *KLF4/Klf4*, *c-MYC/c-Myc* and *RONIN/Ronin* in human/mouse AM cells may function in facilitating the generation efficiency of iPSCs. The human AM cell, which is conventionally freeze-storable, could be a useful cell source for the generation of pluripotent stem cells including iPSCs mediated by nuclear reprogramming in the purpose of personal regenerative and pharmaceutical cure in the future of infants.

Results

Generation of iPSCs from mouse AM and YS cells

Extra-embryonic membranes, AM (amniotic ectoderm and mesoderm layers) and YS (visceral yolk sac endoderm and mesoderm layers) express a high level of proto-oncogene (Curran *et al.* 1984) which function, at least in part, to maintain and protect the fetus in utero. In E18.5 mouse embryos just before birth, AM and YS can be easily recognized microscopically (Fig. 1a). The membranes were dissected from *Oct4-GFP* (OG)/*Neo-LacZ* (Rosa26) embryos as approximately 5–10 mm² sections and digested with collagenase. Isolated cells were cultured for 4–5 days resulting in morphologically heterogeneous populations (Fig. 1a) in which OG expression was undetectable. Approximately 1×10^5 cells were then retrovirally transfected with exogenous *Oct4*, *Sox2*, *Klf4* and *c-Myc* (OSKM). After approximately 3 weeks, OG-positive embryonic stem cell (ESC)-like miPSC colonies were picked and expanded without drug selection. All AM (female) and YS (male)-miPSC lines generated here, which closely resembled ESCs in morphology (Fig. 1a), had a $2n = 40$ normal karyotype (data not shown).

Characterization of AM and YS-miPSCs

As with ESCs, all AM- and YS-miPSC colonies were positive for alkaline phosphatase (ALP) (Fig. 1b).

Immunohistochemical analyses also demonstrated that the cells were positive for pluripotent cell-specific nuclear proteins *Oct4* and *Nanog*, and the surface glycoprotein SSEA1 (Fig. 1b). Thus, the expression profile of all marker proteins tested in AM and YS-miPSCs was similar to that observed in ESCs.

To examine the global transcription profile of these cells, comparative Affymetrix gene expression microarray analyses were performed between AM cells, YS cells, YS-miPSCs and R1 ESCs (Fig. 1c). The global gene expression profile of YS-miPSCs was significantly different from that of YS cells. We detected a similar behavior between AM-miPSCs and AM cells (data not shown). Notably, the profile was similar to that of ESCs (Fig. 1c). Together, the data indicate that significant global nuclear reprogramming had occurred in these cells in response to OSKM transfection. We next applied RT-PCR analysis to gain a more focused transcriptional profile of pluripotent cell-specific marker genes in the induced cells. We found that *Nanog*, *Rex1*, *ERas*, *Gdf3*, *Zfp296* and *Ronin* were expressed in both AM and YS-miPSCs, whereas the AM and YS genes, *Igf1* and *Cd6* were silenced (Fig. 1c). Notably, *Ronin* was expressed not only in AM and YS-miPSCs but also in the precursor AM and YS cells. To investigate whether the exogenous *Oct4*, *Sox2*, *Klf4* and *c-Myc* genes were silenced by DNA methylation as reported for other iPSCs (Jaenisch & Young 2008) in the AM and YS-miPSCs, we examined expression using gene-specific primer sets designed to distinguish endogenous and exogenous transcripts. In all miPSC lines, the expression of endogenous *Oct4*, *Sox2*, *Klf4* and *c-Myc* was similar to that in R1 ESCs, whereas the exogenous *c-Myc* and *Klf4* were fully silenced in some YS-miPSC clones but not in others (Fig. 1c). Notably, high-level expression of endogenous *Klf4* and *c-Myc* was detected even in AM and YS cells, consistent with the expression of proto-oncogene (Curran *et al.* 1984). Endogenous expression of *Klf4*, *c-Myc* and *Ronin* genes that are involved in maintaining pluripotency may play a key function in enhancing the generation efficiency of miPSCs from AM and YS cells.

Timing and efficiency of miPSC generation

The molecular mechanisms that govern OSKM-induced nuclear reprogramming of somatic cells to iPSCs are poorly understood. It has been demonstrated that activation of endogenous *Oct4* may be a landmark for irreversible epigenetic transition toward

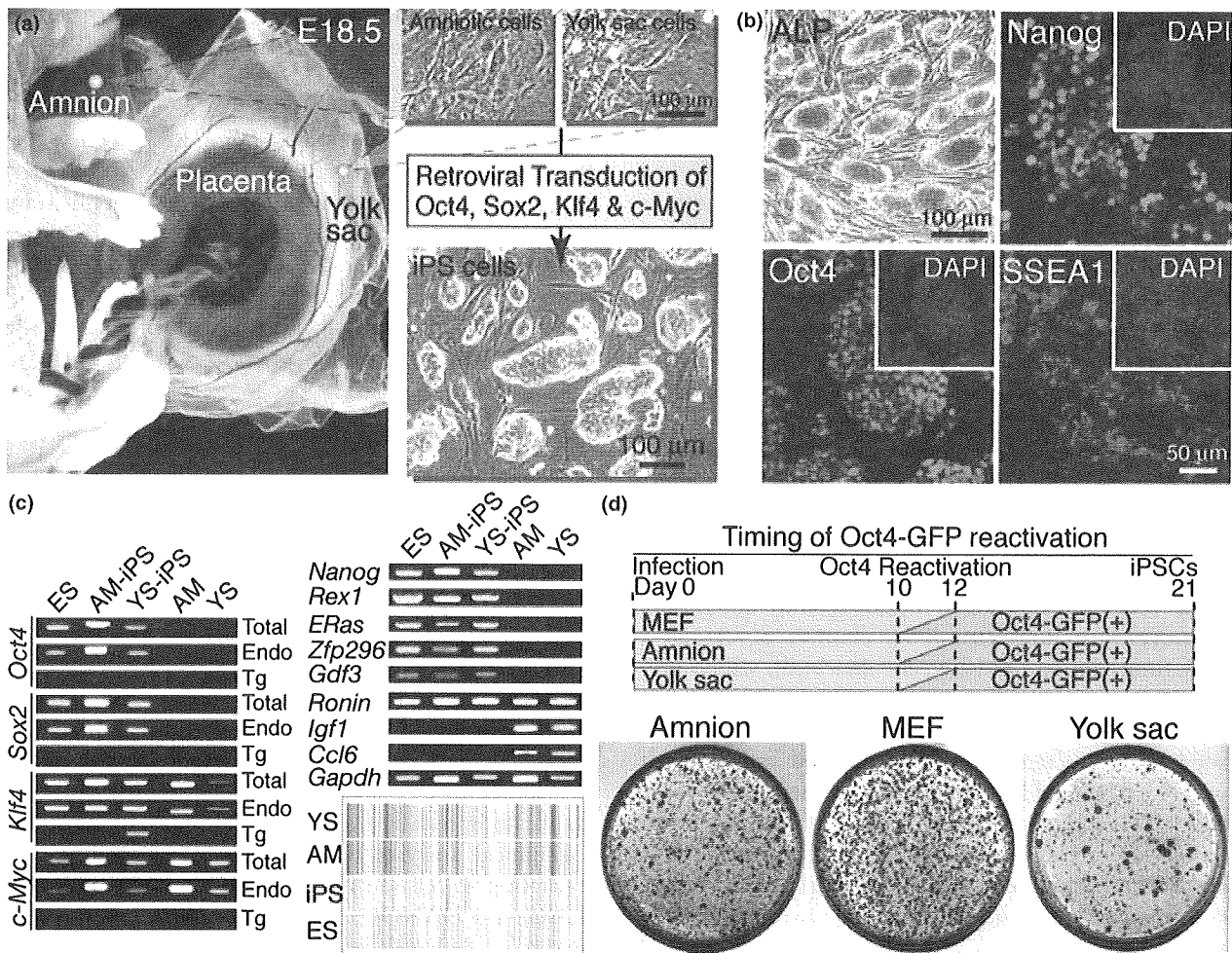


Figure 1 Generation of iPSCs from mouse AM and YS cells. (a) Isolation of AM and YS cells from the extra-embryonic tissues of newborn mice and generation of miPSCs through epigenetic reprogramming by retroviral infection-mediated expression of *Oct4*, *Sox2*, *Klf4* and *c-Myc*. (b) Expression of pluripotent cell marker proteins, alkaline phosphatase (ALP), Nanog, Oct4 and SSEA1. Cell nuclei were visualized with DAPI. (c) Transcriptional activation and silencing of pluripotent and somatic cell marker genes by miPSC induction. RT-PCR analyses revealed that pluripotent marker genes were activated, somatic marker genes were silenced, and *Klf4*, *c-Myc* and *Ronin* were expressed even in AM and YS cells. *Gapdh* is a positive control. Microarray analyses demonstrated global alteration in gene expression profile between YS cells and YS-miPSCs, which more closely resemble mESCs. Relative level of gene expression is illustrated as red > yellow > green. (d) The generation efficiency of ALP-positive colonies and timing of GFP detection demonstrating *Oct4-GFP* reporter gene reactivation. ALP-positive colonies (red) in a 10-cm culture dish was shown when 1.0×10^5 of AM cells, YS cells and MEFs were exposed to OSKM reprogramming factors and reseeded at day 4.

fully reprogrammed iPSCs (Sridharan & Plath 2008). Thus, the timing of reactivation of OG is closely linked with the efficiency of reprogramming. Activation of exogenous OG was detected in some cell populations in every colony around 10 days after OSKM transfection of AM and YS cells, similar to control MEFs examined here and those reported previously (Fig. 1d) (Brambrink *et al.* 2008). The reprogramming efficiency of AM and YS cells was

estimated by ALP-staining 21 days after OSKM transfection with reseeded at day 4. Notably, the number of ALP-positive colonies was similar between AM cells (4373 ± 983 ; mean \pm SEM, $n = 3$) and MEFs (4997 ± 1049 , $n = 3$), and $\sim 50\%$ in YS cells (2293 ± 487 , $n = 3$). Thus, the efficiency of AM reprogramming by OSKM is comparable to that of MEFs, and far exceeds that of adult somatic cells (Fig. 1d).

Germline-transmissible chimeras with AM and YS-miPSCs

To address *in vivo* differentiation potential of the AM and YS-miPSCs, approximately 10 agouti miPSCs were microinjected into C57BL/6J × BDF1 blastocysts (black), and transferred into white ICR foster mothers to generate chimeras. Three male YS-miPSC and two female AM-miPSC lines were tested for chimera formation. X-gal staining analysis on sections of E15.5 embryos demonstrated successful generation of normally developing chimeric embryos with OG/*Neo-LacZ* miPSC contribution to the majority of tissues in all miPSC lines examined (data not shown). We next examined the miPSC potential for normal growth to sexual maturity and germline transmission. Two high-degree chimeric mice with a YS-miPSC line and three high-degree chimeric mice with two AM-miPSC lines, characterized by the >50% contribution of agouti coat color (Fig. 2a), developed normally into adulthood. However, an adult YS-miPSC chimera developed a neck tumor around 8–10 weeks after birth, which may be due to reactivation of the exogenous *c-Myc* as reported previously (Nakagawa *et al.* 2008). Testes isolated from affected males were bisected and one-half was X-gal-stained for LacZ activity whereas the other half was cryosectioned. Blue staining in the seminiferous tubule indicated that YS-miPSCs could contribute to germ cell development. To confirm this, testis cryosections immunohistochemically stained with antibodies against LacZ (iPSC-derived cell marker) and TRA98 (spermatogonia and spermatocyte marker) (Fig. 2b). Germ cells in all tubules were positive for TRA98, whereas germ cells in only some seminiferous tubules were positive for LacZ, clearly demonstrating that YS-miPSCs are capable of contributing to the differentiating germ line in chimeras. Finally, to examine whether the genetic information of YS-miPSCs was transmissible to the next generation, DNA isolated from progeny of the remaining YS-miPSC chimera was analyzed by genomic PCR with a primer set specific to *Neo*. Seven of the thirty-five pups examined were positive, demonstrating that YS-miPSCs are able to differentiate into fully functional germ cells (Fig. 2c). In one of three female AM-miPSC chimeric mice, competence for contribution to germ cells was detected by X-gal staining analysis of ovaries (data not shown).

Teratoma formation with AM and YS-miPSCs

The differentiation competence of AM and YS-miPSCs was further tested by teratoma formation

induced by injection of cells into the inguinal region of immunodeficient SCID mice. Teratomas were isolated 5–8 weeks after for histological analysis and for gene expression analysis. Hematoxylin–eosin (HE) staining of paraffin sections demonstrated that the three primary layers were generated as morphologically shown by ectodermal glia and neuroepithelium, mesodermal muscle and endodermal ciliated epithelium and cartilage (Fig. 2d). Multi-lineage differentiation of miPSCs was verified by transcription of endodermal, mesodermal and ectodermal genes in the majority of teratomas (Fig. 2e).

Generation of iPSCs from human AM cells

To examine whether hiPSCs could be efficiently generated from primary AM cells isolated from the amniotic membrane ($\sim 100\text{ cm}^2$) of the placenta of newborn human (Fig. 3a), the reprogramming factors *OCT4*, *SOX2*, *KLF4* and *c-MYC* were introduced by vesicular stomatitis virus G glycoprotein (VSV-G) retroviral transduction. About 20 AM-hiPSC lines were established from 1.0×10^5 AM cells infected (0.02%). The efficiency of AM-hiPSC generation is markedly high relative to that with cells from human adult tissues (Yu *et al.* 2007). AM-hiPSCs were morphologically similar to human ESCs (hESCs) (Fig. 3a). Immunohistochemical analyses demonstrated expression of the pluripotent cell-specific nuclear proteins *OCT4*, *SOX2* and *NANOG*, and the keratan sulfate proteoglycan TRA-1-60 (Fig. 3b) consistent with the profile observed in hESCs. To extend this analysis, we examined the expression profile of genes by RT-PCR. The endogenous reprogramming factor genes *OCT4*, *SOX2*, *KLF4* and *c-MYC* were all activated in AM-hiPSCs, whereas the transgenes were fully silenced (Fig. 3c). Expression of pluripotent cell-specific genes *NANOG*, *REX1*, *GDF3*, *ESG1*, *FGF4*, *TERT* and *RONIN* were also activated in all AM-hiPSC clones consistent with the profile of control hESCs (Fig. 3c). Notably, transcription of *KLF4*, *c-MYC*, and *RONIN* was detected not only in AM-hiPSCs but also AM cells. Similar to mouse AM and YS cells, endogenous expression of *KLF4*, *c-MYC* and *RONIN* in human AM cells may facilitate acquisition of reprogramming competency for efficient generation of hiPSCs.

DNA methylation of *OCT4* and *NANOG* in AM-hiPSCs

To further characterize the pluripotent nature of AM-hiPSCs, the promoter CpG methylation status

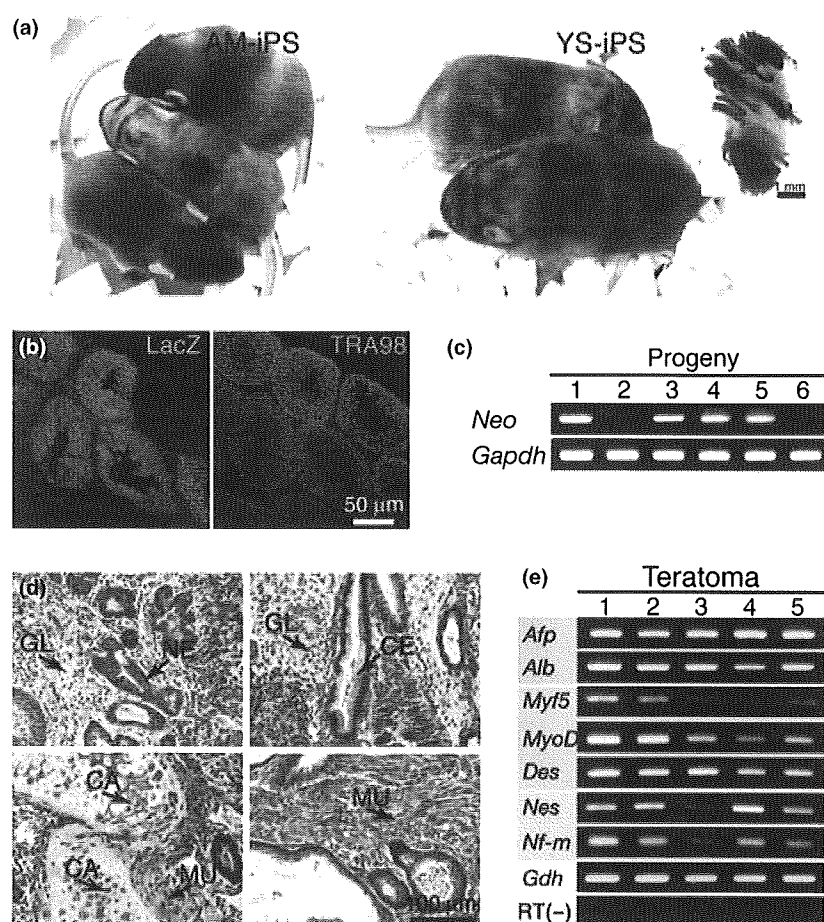


Figure 2 Pluripotency of AM and YS-miPSCs. (a) Chimeric mice with female AM-miPSCs and male YS-miPSCs. Inset: X-gal staining of testis collected from an adult YS-miPSC chimera (blue cells are YS-miPSC derivatives). (b) Immunohistochemical double staining of testis cryosections from a YS-miPSC chimera with anti-LacZ (YS-miPSC-derived germ cells) and anti-TRA98 (spermatogonia and spermatocytes) antibodies. (c) Genotyping of progeny obtained by backcrossing with YS-miPSC chimeras. *Neo* positive demonstrates germline transmission of YS-miPSC genetic information. *Gapdh* is positive control. (d) Hematoxylin-eosin staining of teratoma sections generated by AM and YS-miPSC implantation. GL, glia (ectoderm); NE, neuroepithelium (ectoderm); CE, ciliated epithelium (endoderm); CA, cartilage (ectoderm); MU, muscle (mesoderm). (e) Transcription analysis of lineage-specific genes in teratomas generated with AM and YS-miPSCs. Gray rectangle: endoderm makers; purple rectangle: mesoderm markers; pink rectangle: ectoderm markers. *Afp*, α -Fetoprotein; *Alb*, albumin; *Des*, desmin; *Nes*, Nestin; *Nf-m*, neurofilament-M; *Gdh*, *Gapdh* (positive control).

of key pluripotency genes was examined by bisulfite-modified DNA sequencing. Promoters of both *OCT4* and *NANOG* were found to highly methylated in hAM cells, consistent with transcriptional silencing in these cells. Conversely, both promoter regions were hypo-methylated in AM-hiPSCs consistent with the observed reactivation (Fig. 3d). These data demonstrate that human AM cells are capable of being epigenetically reprogrammed to AM-hiPSCs through forced expression of reprogramming factors.

Teratoma formation with AM-hiPSCs

To address whether the AM-hiPSCs have competence to differentiate into specific tissues, teratoma formation was induced by implantation under the kidney capsule of immunodeficient nude mice. Twenty-one out of twenty-four AM-hiPSC independent clones induced teratoma formation within 6–10 weeks of implantation (1.0×10^7 cells/site). Histological analysis by HE staining of paraffin-embedded sections demonstrated that the three

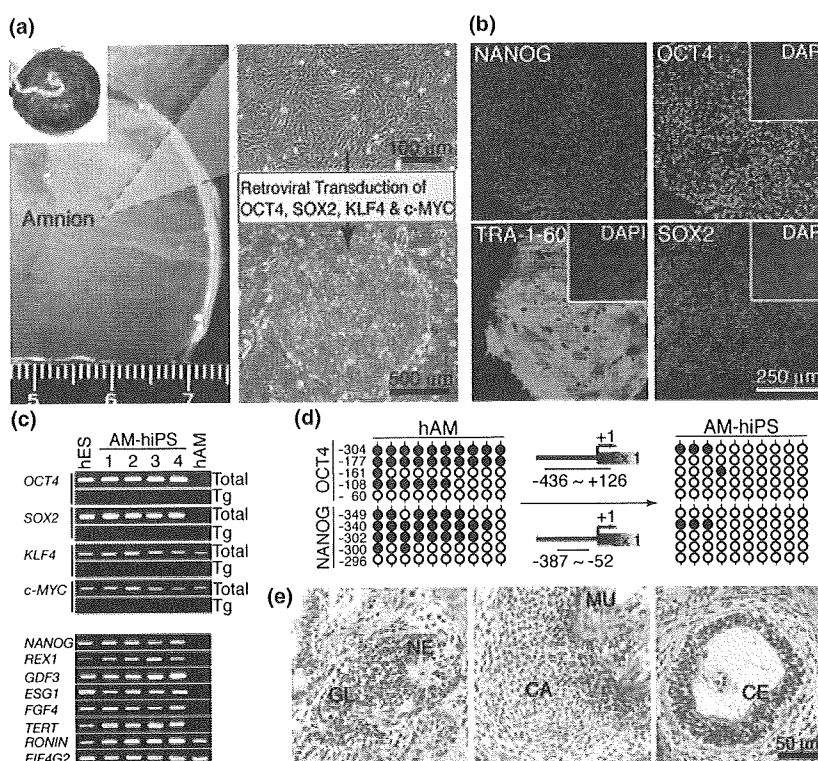


Figure 3 Generation of iPSCs from human AM cells. (a) Isolation of hAM cells from extra-embryonic tissues of human newborns and generation of hiPSCs through epigenetic reprogramming by retroviral infection-mediated expression of *OCT4*, *SOX2*, *KLF4* and *c-MYC*. (b) Expression of pluripotent cell marker proteins, NANOG, OCT4, TRA-1-60 and SOX2. Cell nuclei were visualized with DAPI. (c) Transcriptional activation of pluripotent marker genes by hiPSC induction. RT-PCR analyses revealed that the exogenous *OCT4*, *SOX2*, *KLF4* and *c-MYC* genes were silenced and the endogenous pluripotent marker genes were activated in AM-hiPSCs. *KLF4*, *c-MYC* and *RONIN* were expressed even in hAM cells before reprogramming. *EIF4G2* (*eukaryotic translation initiation factor 4 gamma 2*) is included as a positive control. (d) Epigenetic reprogramming of the *OCT4* and *NANOG* promoter regions. Bisulfite-modified DNA sequence analysis demonstrated a transition from hyper-methylation in AM cells (black circles) to hypo-methylation in AM-hiPSCs (white circles). (e) Hematoxylin-eosin staining of teratoma sections of teratoma generated by AM-hiPSC implantation. GL, glia (ectoderm); NE, neuroepithelium (ectoderm); CE, ciliated epithelium (endoderm); CA, cartilage (ectoderm); MU, muscle (mesoderm).

primary layers were generated as shown by ectodermal glia and neuroepithelium, mesodermal muscle and endodermal ciliated epithelium and cartilage morphologically (Fig. 3e). Thus, the majority of AM-hiPSC clones have potential for multi-lineage differentiation *in vivo*.

Discussion

We here demonstrated that hiPSCs and miPSCs were efficiently generated from newborn AM cells, in which endogenous *Klf4*, *c-Myc* and *Ronin* were highly expressed. The generation efficiency of miPSCs from AM cells was comparable to that from MEFs in mice and was notably high to that from adult somatic cells in humans. The properties of AM-hiPSCs and AM or

YS-miPSCs resemble those of fully reprogrammed iPSCs from other tissues and ESCs.

iPSCs are generated through epigenetic reprogramming of somatic cells. Information on the base sequence of DNA in nuclei is unchanged through the reprogramming, although the gene expression profile is altered through the reprogramming from the somatic cell to the iPSC type. Developmentally rewound iPSCs retain aged DNA base sequence information inherited from somatic cells. The base sequence of DNA accumulates mutations through aging with cell division and mis-repair. Young somatic cells are suitable for iPSC generation rather than aged somatic cells. Therefore, it is suggested that the AM cells accumulating less genetic mutation are safer than the adult somatic cells as a cell source for iPSC generation.

The generation efficiency of OG-positive colonies was approximately four times lower than that of ALP-positive colonies and it is likely that miPSC generation will be further reduced (Wernig *et al.* 2008). Furthermore, when pre-iPSCs are reseeded, the generation efficiency of iPSC outcome could be roughly estimated as $1/2^X$ (X = reseeded day after infection or transfection; doubling time of pre-iPSC is estimated as 24 h). Recently, iPSC generation technology has been developed and improved with MEFs and human embryonic or newborn fibroblasts (HNFs) as representative somatic cells. Even with these types of cells, application of the current technology resulted in a marked decrease in iPSC generation efficiency. The retroviral transduction-mediated miPSC generation efficiency is 0.05–0.1% with MEFs (Takahashi *et al.* 2007; Wernig *et al.* 2007). The generation efficiency of hiPSCs ($\sim 0.01\%$ in ALP-positive colony and 0.0025% in hiPSC outcome) (Yu *et al.* 2007; Wernig *et al.* 2008) is ~ 10 times lower than that of miPSCs. The generation efficiency of genetic modification-free hiPSCs from HNFs by direct delivery of reprogramming proteins is estimated at about 0.001% in outcome (Kim *et al.* 2009). Notably, it is evident that the generation of hiPSCs from adult somatic cells is much harder than that from MEFs. In fact, analysis with a secondary dox-inducible transgene system shows that the efficiency varies between different somatic cell types (Wernig *et al.* 2008). Thus, for practical application of iPSC technology to medical care, identification of reprogramming-sensitive cell types is a key issue. Human primary keratinocytes are one candidate cell type for efficient generation of hiPSCs from adult patients (the efficiency of ALP-positive colony = 1.0%) (Aasen *et al.* 2008). Here, we have shown that human and mouse AM cells, in which the endogenous *KLF4/Klf4*, *c-MYC/c-Myc* and *RONIN/Ronin* are naturally expressed, are highly reprogramming-sensitive (hiPSC generation efficiency was approximately 0.02% in outcome). An important point is that relatively huge amounts of human AM cells can be collected from discarded AM membranes at birth with no risk to the individual. Furthermore, these cells can be kept in long-term storage without requirement for amplification by in vitro cell culture.

Our findings illustrate that human AM cells are a strong candidate cell source for collection and banking that could be retrieved on demand and used for generating personalized genetic modification-free iPSCs applicable for clinical treatment and drug screening.

Experimental procedures

Amnion and yolk sac cells

In mice, AM and YS membranes collected from E18.5 embryos from GOF-18/delta PE/GFP (Oct4-GFP) transgenic females (Yoshimizu *et al.* 1999) mated with 129/Rosa26 transgenic males (Friedrich & Soriano 1991) were digested with 0.1% collagenase (Wako, Osaka, Japan) and 20% fetal bovine serum (FBS) at 37 °C for 1 h, and then repeatedly passed through a 26-gauge needle. The cell suspension was cultured with mES medium (DMEM/F12 (Dulbecco's modified Eagle's medium/Ham's F12) (Wako) supplemented with 15% FBS, 10^{-4} M 2-mercaptoethanol (Sigma) and 1000 U/mL of recombinant leukemia inhibitory factor (Chemicon, Temecula, CA, USA) containing 5 ng/mL basic fibroblast growth factor (bFGF) (Peprotech, Rocky Hill, NJ, USA). Following culture for 2–3 days, the adherent AM and YS cells growing to near-confluence were applied for iPSC experiments.

In humans, the AM membrane was cut into tiny pieces with dissection scissors. The AM membrane pieces were cultured in DMEM with 10% FBS for 7–10 days. The adherent AM cells growing to near-confluence were applied for iPSC experiments. Primary AM cells were provided from the cell bank of RIKEN Bioresource Center, Japan.

Generation of iPSCs

In mouse, each of pMXs-Oct4, Sox2, Klf4, c-Myc and DsRed (an indicator of retroviral silencing) was transfected into the Plat-E cells using the FuGENE6 Transfection Reagent (Roche Diagnostics, Indianapolis, IN, USA). A 1 : 1 : 1 : 1 : 4 mixture of Oct4, Sox2, Klf4, c-Myc and DsRed retroviruses in supernatants with 4 µg/mL polybrene (Nacalai Tesque, Kyoto, Japan) was added to AM and YS cells at 1.0×10^5 cells per 3 cm well. At day 4 after infection, the cells were reseeded into a 10 cm culture dish on feeder cells with mES medium. Colonies were picked around day 20.

In humans, pMXs-OCT4, SOX2, KLF4 or c-MYC, pCL-GagPol, and pHCMV-VSV-G vectors were transfected into 293FT cells (Invitrogen, Carlsbad, CA, USA) using the TransIT-293 reagent (Mirus). A 1 : 1 : 1 : 1 mixture of OCT4, SOX2, KLF4 and c-MYC viruses in supernatant with 4 µg/mL polybrene were added to AM cells at 1.0×10^5 cells per 3 cm well. The cells were subcultured on feeder cells into a 10 cm dish with the iPSellon medium (Cardio) supplemented with 10 ng/mL bFGF (Wako) (hES medium). Colonies were picked up around day 28.

Immunocytochemistry

Human and mouse cells were fixed with 4% paraformaldehyde in phosphate-buffered saline (PBS) for 10 min at 4 °C. After washing with 0.1% Triton X-100 in PBS (PBST), the cells were prehybridized with blocking buffer for 1–12 h at 4 °C and then incubated with primary antibodies; anti-SSEA4

Table 1 Primers for RT-PCR and PCR

Gene name	5'-Forward-3'	5'-Reverse-3'
Mice		
<i>Oct4</i> (total)	CTGAGGGCCAGGCAGGAGCACGAG	CTGTAGGGAGGGCTTCGGGCACTT
<i>Oct4</i> (endogenous)	TCTTTCCACCAGGCCCCCGGCTC	TGCGGGCGGACATGGGGAGATCC
<i>Oct4</i> (transgene)	CCCATGGTGGTGGTACGGGAATTC	AGTTGCTTTCCACTCGTGCT
<i>Sox2</i> (total)	GGTTACCTCTTCCCTCCACTCCAG	TCACATGTGCGACAGGGGCAG
<i>Sox2</i> (transgene)	CCCATGGTGGTGGTACGGGAATTC	TCTCGGTCTCGGACAAAAGT
<i>Klf4</i> (total)	CACCATGGACCCGGGCGTGGCTGCCAGAAA	TTAGGCTGTTCTTTTCCGGGGCCACGA
<i>Klf4</i> (endogenous)	GCGAACTCACACAGGCGAGAAACC	TCGCTTCCTCTTCCCTCCGACACA
<i>Klf4</i> (transgene)	CCCATGGTGGTGGTACGGGAATTC	GTCGTTGAACTCCTCGGTCT
<i>c-Myc</i> (total)	CAGAGGAGGAACGAGCTGAAGCGC	TTATGCACCAGAGTTTTCGAAGCTGTTTCG
<i>c-Myc</i> (endogenous)	CAGAGGAGGAACGAGCTGAAGCGC	AAGTTTGAGGCAGTTAAAATTATGGCTGAAGC
<i>c-Myc</i> (transgene)	CTCCTGGCAAAAAGGTCAGAG	GACATGGCCTGCCCGGTTATTATT
<i>Nanog</i>	ATGAAGTGC AAGCGGTGGCAGAAA	CCTGGTGGAGTCACAGAGTAGTTC
<i>Eras</i>	CAAAGATGCTGGCAGGCAGCTACC	GACAAGCAGGGCAAAGGCTTCCCTC
<i>Gdf3</i>	AGTTTCTGGGATTAGAGAAAAGC	GGGCCATGGTCAACTTTGCTT
<i>Rex1</i>	GACATCATGAATGAACAAAAAATG	CCTTCAGCATTCTTCCCTG
<i>Zfp296</i>	AAGCACCCAGATCTGTTGACCT	GAGCCTCTGGGGTATCTAGG
<i>Ronin</i>	GCCTCAGAGCTAGAGGCTGCTACG	TGGAAGGAGTCACGAATTCTGCAG
<i>Igf1</i>	GGACCAGAGACCCTTTGCGGGG	GGCTGCTTTTGTAGGCTTCAGTGG
<i>Ccl6</i>	CCTAAGCACCCCTGAAGCAAG	ACAACTGGGAACCCACAAAAGC
<i>Gapdh</i>	CCCCTAACATCAAATGGGG	CCTTCCACAATGCCAAAGTT
<i>α-Fetoprotein</i>	TCGTATTCCAACAGGAGG	CACTCTCCTTCTGGAGATG
<i>Albumin</i>	AAGGAGTCTGCCATGGTGA	CCTAGGTTTCTTGCAGCCTC
<i>Myf-5</i>	TGCCATCCGCTACATTGAGAG	CCGGGTAGCAGGCTGTGAGTTG
<i>MyoD</i>	GCCCGCGCTCCAACCTGCTCTGAT	CCTACGGTGGTGCGCCCTCTGC
<i>Desmin</i>	TTGGGGTCTGCTGCGGTCTAGCC	GGTCGTCTATCAGGTTGTCACG
<i>Nestin</i>	GGAGTGTCTGCTTAGAGGTGC	TCCAGAAAGCCAAGAGAAGC
<i>Neurofilament-M</i>	GCCGAGCAGACCAAGGAGGCCATT	CTGGATGGTGTCTTGGTAGCTGCT
<i>Neo</i>	CGGCAGGAGCAAGGTGAGAT	CAAGATGGATTGCACGCAGG
Humans		
<i>OCT4</i> (total)	GCCGTATGAGTTCTGTGG	TCTCCTTCTCCAGCTTCAC
<i>SOX2</i> (total)	TAAGTACTGGCGAACCATCT	AAATTACCAACGGTGTCAAC
<i>KLF4</i> (total)	ACTCGCCTTGCTGATTGTCT	GAACGTGGAGAAAGATGGGA
<i>c-MYC</i> (total)	GCGTCTGGGAAGGGAGATCCGGAGC	TTGAGGGGCATCGTCGCGGGAGGCTG
<i>NANOG</i>	ATTATGCAAGCAACTCACTT	GATTCTTTACAGTCGGATGC
<i>REX1</i>	CAGATCCTAAACAGCTCGCAGAAT	GCGTACGCAAATTAAGTCCAGA
<i>GDF3</i>	CTTATGCTACGTAAGGAGCGGG	GTGCCAACCCAGGTCCCGGAAGTT
<i>ESG1</i>	ATATCCC GCCGTGGGTGAAAGTTC	ACTCAGCCATGGACTGGAGCATCC
<i>FGF4</i>	CTACAACGCCTACGAGTCTTACA	GTTGCACCAGAAAAGTCAGAGTTG
<i>TERT</i>	CCTGCTCAAGCTGACTCGACACCGTG	GGAAAAGCTGGCCCTGGGGTGGAGC
<i>RONIN</i>	CACTGTAGACAGCAGTCAGG	TGCCTTTCATCTCTTTCATC
<i>EIF4G2</i>	AAGGAAAGGGACTGAGTTTC	CCAAGAAAGCTTCTTCTTCA
<i>Bis-OCT4</i>	GATTAGTTTGGGTAATATAGTAAAGT	ATCCCACCCACTAACCTTAACCTCTA
<i>Bis-NANOG</i>	TGGTTAGGTTGGTTTTAAATTTTTG	AACCCACCCTTATAAATTCTCAATTA

(1 : 300) (Chemicon), anti-TRA-1-60 (1 : 300) (Chemicon), anti-Oct4 (1 : 50) (Santa Cruz Biotechnology, Santa Cruz, CA, USA), anti-Nanog (1 : 300) (ReproCELL, Tokyo, Japan), anti-Sox2 (1 : 300) (Abcam, Cambridge, UK) and/or anti-SSEA1 (1 : 1000) (DSHB) antibodies for 6–12 h at 4 °C. They were incubated with secondary antibodies; anti-rabbit

IgG, anti-mouse IgG or anti-mouse IgM conjugated with Alexa 488 or 546 (1 : 500) (Molecular Probes, Eugene, OR, USA) in blocking buffer for 1 h at room temperature. The cells were counterstained with 4,6-diamidino-2-phenylindole (DAPI) and then mounted with a SlowFade light antifade kit (Molecular Probes). To examine germline competence,

cryosections of a half of a testis of 4- to 5-week-old chimeric mice were fixed with 4% paraformaldehyde in PBS for overnight at 4 °C, and then prehybridized with blocking buffer. The sections were double-stained with primary antibodies; anti-LacZ antibody (1 : 500) (Promega, Madison, WI, USA) specific to miPSC-derived cells and with anti-TRA98 antibody (1 : 500) specific to spermatogonia and spermatocytes. The remaining testis and ovaries were stained with X-gal.

RT-PCR

Total RNAs were isolated from mouse and human cells using the TRIzol (Invitrogen) and the RNeasy Plus Mini Kit (Qiagen, Valencia, CA, USA), respectively. cDNAs were synthesized from 1 µg total RNAs using Superscript III reverse transcriptase (Invitrogen) with random hexamers according to the manufacturer's instructions. Template cDNA was PCR-amplified with gene-specific primer sets (Table 1).

Gene expression microarray

Total RNA was extracted from mouse cells using the TRIzol Reagent. Double-stranded cDNA synthesized from the total RNA was amplified and labeled using the One-Cycle Target Labeling and Control Regents (Affymetrix, Santa Clara, CA, USA). Global gene expression was examined with the GeneChip Mouse Genome 430 2.0 Array (Affymetrix). The fluorescence intensity of each probe was quantified by using the GeneChip Analysis Suite 5.0 computer program (Affymetrix). The level of gene expression was determined as the average difference (AD). Specific AD levels were then calculated as percentages of the mean AD level of probe sets for housekeeping genes *Actin* and *Gapdh*. To eliminate changes within the range of background noise and to select the most differentially expressed genes, data were used only if the raw data values were less than 50 AD. Further data were analyzed with GeneSpring GX 7.3.1 (Agilent Technologies, Santa Clara, CA, USA).

Reprogramming efficiency

The reprogramming efficiency of mouse YS and AM cells was estimated by counting the number of ALP-positive colonies 21 days after retroviral infection. The cells in 10 cm culture dish were fixed with 4% paraformaldehyde in PBS for 15 min at room temperature and washed with PBS. After treating with ALP stain (pH 9.0) for 30 min at room temperature, the number of ALP-positive cells was counted.

Chimera

AM-miPSCs ($2n = 40$, XX) and YS-miPSCs ($2n = 40$, XY) were microinjected into blastocysts (C57BL/6J × BDF1). The blastocysts were transferred into the uterus of pseudopregnant ICR female mice. Chimeric mice were mated with C57BL/6J

for examining germline transmission. The genotype of the progeny was determined with tail tip DNA by genomic PCR with a *Neo*-specific primer set (Table 1). All animal experiments were performed according to the guidelines of animal experiments of Kyoto University, Japan.

Teratoma

In mice, cell suspension of 1.0×10^6 AM or YS-miPSCs/100 µL DMEM/F12 was subcutaneously injected into the inguinal region of immunodeficient SCID mice (CLEA). In humans, the 1 : 1 mixture of the AM-hiPSC suspension and Basement Membrane Matrix (BD Biosciences, San Jose, CA, USA) were implanted at 1.0×10^7 cells/site under the kidney capsule of immunodeficient nude mice (CLEA). Teratomas surgically dissected out 5–8 weeks in mice and 6–10 weeks in human after implantation, were fixed with 4% paraformaldehyde in PBS, and embedded in paraffin. Sections at 10 µm in thickness were stained with HE.

Bisulfite-modified DNA sequencing

Genomic DNAs (1 µg) extracted from AM-hiPSCs and hAM cells were bisulfite-treated with EZ DNA methylation-Gold Kit (ZYMO Research, Orange, CA, USA) according to the manufacturer's instruction. The promoter regions of the human *NANOG* and *OCT4* genes were PCR-amplified with specific primer sets (Table 1). Ten clones of each PCR product were gel-purified, sub-cloned and sequenced with the SP6 universal primer.

Acknowledgements

We thank Dr Gen Kondoh and Miss Hitomi Watanabe for generating chimeras, and Dr Justin Ainscough for critical comments on the manuscript.

References

- Aasen, T., Raya, A., Barrero, M.J., Garreta, E., Consiglio, A., Gonzalez, F., Vassena, R., Bilic, J., Pekarik, V., Tiscornia, G., Edel, M., Boue, S. & Belmonte, J.C. (2008). Efficient and rapid generation of induced pluripotent stem cells from human keratinocytes. *Nat. Biotechnol.* **26**, 1276–1284.
- Brambrink, T., Foreman, R., Welstead, G.G., Lengner, C.J., Wernig, M., Suh, H. & Jaenisch, R. (2008). Sequential expression of pluripotency markers during direct reprogramming of mouse somatic cells. *Cell Stem Cell* **2**, 151–159.
- Curran, T., Miller, A.D., Zokas, L. & Verma, I.M. (1984). Viral and cellular fos proteins: a comparative analysis. *Cell* **36**, 259–268.
- Feng, B., Ng, J.H., Heng, J.C. & Ng, H.H. (2009). Molecules that promote or enhance reprogramming of somatic cells to induced pluripotent stem cells. *Cell Stem Cell* **4**, 301–312.

- Friedrich, G. & Soriano, P. (1991). Promoter traps in embryonic stem cells: a genetic screen to identify and mutate developmental genes in mice. *Genes Dev.* **5**, 1513–1523.
- Jaenisch, R. & Young, R. (2008). Stem cells, the molecular circuitry of pluripotency and nuclear reprogramming. *Cell* **132**, 567–582.
- Kim, D., Kim, C.H., Moon, J.I., Chung, Y.G., Chang, M.Y., Han, B.S., Ko, S., Yang, E., Cha, K.Y., Lanza, R. & Kim, K.S. (2009). Generation of human induced pluripotent stem cells by direct delivery of reprogramming proteins. *Cell Stem Cell* **4**, 472–476.
- Nakagawa, M., Koyanagi, M., Tanabe, K., Takahashi, K., Ichisaka, T., Aoi, T., Okita, K., Mochiduki, Y., Takizawa, N. & Yamanaka, S. (2008). Generation of induced pluripotent stem cells without Myc from mouse and human fibroblasts. *Nat. Biotechnol.* **26**, 101–106.
- Sridharan, R. & Plath, K. (2008). Illuminating the black box of reprogramming. *Cell Stem Cell* **2**, 295–297.
- Takahashi, K., Okita, K., Nakagawa, M. & Yamanaka, S. (2007). Induction of pluripotent stem cells from fibroblast cultures. *Nat. Protoc.* **2**, 3081–3089.
- Wernig, M., Lengner, C.J., Hanna, J., Lodato, M.A., Steine, E., Foreman, R., Staerk, J., Markoulaki, S. & Jaenisch, R. (2008). A drug-inducible transgenic system for direct reprogramming of multiple somatic cell types. *Nat. Biotechnol.* **26**, 916–924.
- Wernig, M., Meissner, A., Foreman, R., Brambrink, T., Ku, M., Hochedlinger, K., Bernstein, B.E. & Jaenisch, R. (2007). In vitro reprogramming of fibroblasts into a pluripotent ES-cell-like state. *Nature* **448**, 318–324.
- Yamanaka, S. (2007). Strategies and new developments in the generation of patient-specific pluripotent stem cells. *Cell Stem Cell* **1**, 39–49.
- Yoshimizu, T., Sugiyama, N., De Felice, M., Yeom, Y.I., Ohbo, K., Masuko, K., Obinata, M., Abe, K., Scholer, H.R. & Matsui, Y. (1999). Germline-specific expression of the Oct-4/green fluorescent protein (GFP) transgene in mice. *Dev. Growth Differ.* **41**, 675–684.
- Yu, J., Vodyanik, M.A., Smuga-Otto, K., Antosiewicz-Bourget, J., Frane, J.L., Tian, S., Nie, J., Jonsdottir, G.A., Ruotti, V., Stewart, R., Slukvin, I.I. & Thomson, J.A. (2007). Induced pluripotent stem cell lines derived from human somatic cells. *Science* **318**, 1917–1920.
- Zhou, H., Wu, S., Joo, J.Y., Zhu, S., Han, D.W., Lin, T., Trauger, S., Bien, G., Yao, S., Zhu, Y., Siuzdak, G., Scholer, H.R., Duan, L. & Ding, S. (2009). Generation of induced pluripotent stem cells using recombinant proteins. *Cell Stem Cell* **4**, 381–384.

Received: 20 August 2009

Accepted: 16 September 2009

羊膜から効率よく iPS 細胞

京都大などのグループ発表

胎児を包む羊膜を使って効率よく iPS (人工多能性幹) 細胞をつくることに、京都大再生医学研究所の多田高准教授らが成功し、16日に専門誌に発表した。ヒトでもマウスでも確認された。羊膜は長く保存できるため、将来構想される iPS 細胞バンクで使用する細胞の候補になる可能性がある。同研究所の山中伸弥教授や国立成育医療センター研究所との共同研究。

iPS 細胞は、体細胞に四つの遺伝子を入れてつくる。多田准教授らは、羊膜の細胞では 2 遺伝子がすでに働いていることに注目した。羊膜の細胞に 4 遺伝子を組み込んで iPS 細胞をつくったところ、大人の体の細胞からつくるとより、iPS 細胞ができる率は 10 倍以上となり、効率よくできた。

iPS 細胞の作製効率を高める方法としては、特定の遺伝子の働きを抑えたり、化学物質を使ったりするなどの報告があるが、羊膜からつくる方法はより操作が少なく済むという。多田准教授は「出産時に胎盤と一緒に出てる羊膜を保存し、必要になったとき iPS の細胞をつくるという応用が考えられる」と話している。(瀬川茂子)

Shortening of Human Cell Life Span by Induction of p16ink4a Through the Platelet-Derived Growth Factor Receptor β

HIDEKAZU TAKAHASHI,^{1,2} MASASHI TOYODA,¹ JUN-ICHI BIRUMACHI,¹ AKANE HORIE,¹ TARO UYAMA,¹ KENJI MIYADO,¹ KENJI MATSUMOTO,³ HIROHISA SAITO,³ AND AKIHIRO UMEZAWA^{1*}

¹Department of Reproductive Biology, National Institute for Child Health and Development, Tokyo, Japan

²Tsuruga Institute of Biotechnology, TOYOBO Co. Ltd., Tsuruga, Fukui, Japan

³Department of Allergy and Immunology, National Institute for Child Health and Development, Tokyo, Japan

Mesenchymal stem cells (MSCs) are attracting a great deal of attention because they represent a valuable source of cells for use in regenerative medicine. In human cell culture it is important to obtain large numbers of cells for use in therapy. In this study, we attempted to prolong life span of a marrow-derived mesenchymal stem cell using a combination of growth factors and hormones. Furthermore we tested whether chemically defined culture conditions are sufficient for maintenance of multipotent mesenchymal stem cells. Epidermal growth factor, platelet-derived growth factor-BB (PDGF-BB), acidic fibroblast growth factor (FGF), basic FGF, and leukemia inhibitory factor were found to be key factors for the mesenchymal stem cell proliferation. The combination of these growth factors showed extremely strong mitogenic activity, and simultaneously induced the expression of cyclin-dependent kinase inhibitor p16ink4a protein and premature senescence more rapidly than serum-supported culture conditions. The induction of p16ink4a by growth factors was mediated through the mitogen-activated protein kinase (MAPK) cascade. Excess growth stimulation by growth factors was thus one of the culture stress signals and a trigger of premature senescence at least in human cells.

J. Cell. Physiol. 221: 335–342, 2009. © 2009 Wiley-Liss, Inc.

Bone marrow-derived mesenchymal stem cells, which provide a physical scaffold for hematopoiesis, differentiate into osteoblasts, chondrocytes, skeletal myocytes, adipocytes, and cardiomyocytes in vitro (Pittenger et al., 1999). Moreover, recent studies suggest that bone marrow-derived mesenchymal stem cells can differentiate into a neuronal lineage in addition to cells of mesodermal origin (Mori et al., 2005). Since the use of bone marrow-derived mesenchymal stem cells entails no ethical or immunological problems, they are considered a useful source of cells for transplantation. The phenotype of mesenchymal stem cells can be maintained in cultivation, and are recognized as adherent fibroblastic cells and spindle shaped (Umezawa et al., 1992). Mesenchymal stem cells have been shown to display a considerable therapeutic potential in pre-clinical (Kopen and Phinney, 1999; Petite et al., 2000; Mahmood et al., 2004; Jaquet et al., 2005; Lange et al., 2005; Tögel et al., 2005) and clinical (Horwitz et al., 1999; Koç et al., 2000, 2002; Chen et al., 2004; Le Blanc et al., 2004) studies for treatment of neuronal degeneration, osteogenesis imperfecta, graft versus host diseases, support of hematopoietic engraftment, metabolic diseases, bone and cartilage tissues, as well as renal and myocardial infarction.

In clinical applications of mesenchymal stem cells, it is important not only to remove animal serum from the culture medium for reasons of medical safety with respect to infectious disease (Lennon et al., 1995; Wiles and Johansson, 1999; Yao et al., 2004), but also to obtain large numbers of cells for injection into damaged sites in humans. The cells must be propagated in vitro to obtain large numbers of cells; however, Hayflick's problem is unavoidable in normal cells (Hayflick and Moorhead, 1961; Campisi, 2001). That is, most vertebrate cells stop dividing after a finite number of cell divisions in culture, a process called "senescence" (Wei and Sedivy, 1999; Campisi, 2001). Marrow-derived mesenchymal cells divide

approximately 25–40 times in culture before they cease dividing or reach senescence (Mori et al., 2005). Senescence is classified into two categories: "stress-induced premature senescence" or "telomere-independent senescence" and "replicative senescence" or "telomere-dependent senescence" (Rheinwald et al., 2002; Beausejour et al., 2003). p16ink4a, a cyclin-dependent kinase inhibitor is up-regulated in senescent cells (Hara et al., 1996; Serrano, 1997). This upregulation is directly linked to the increase of the number of cell doublings (Alcorta

Hidekazu Takahashi, Masashi Toyoda, and Jun-ichi Birumachi contributed equally to this work.

Additional Supporting Information may be found in the online version of this article.

Contract grant sponsor: Ministry of Education, Culture, Sports, Science and Technology of Japan;
Contract grant number: KAKENHI 14657051.

Contract grant sponsor: Japan Health Sciences Foundation;
Contract grant number: KH71064.

Contract grant sponsor: The Research Grant for Cardiovascular Diseases;

Contract grant number: H16C-6.

Contract grant sponsor: Grant for Child Health and Development;
Contract grant number: H15C-2.

*Correspondence to: Akihiro Umezawa, Department of Reproductive Biology, National Institute for Child Health and Development, 2-10-1 Okura, Setagaya-ku, Tokyo 157-8535, Japan.
E-mail: umezawa@1985.jukuin.keio.ac.jp

Received 14 October 2008; Accepted 14 May 2009

Published online in Wiley InterScience
(www.interscience.wiley.com.), 6 July 2009.
DOI: 10.1002/jcp.21860

et al., 1996). Inhibition of the p16/Rb pathway is sufficient to prolong the life span of cells in cultures of marrow-derived cells (Mori et al., 2005). Alleviation of culture stress is thus necessary to prolong the life span of mesenchymal cells.

Mesenchymal stem cells have been cultivated in medium supplemented with fetal calf serum (FCS). FCS, however, is an undesired source of xenogeneic antigens (Martin et al., 2005) and bears the risk of transmitting animal viral, prion, and zoonose contaminations. Additionally, FCS has been implicated in anaphylactic immune reactions in patients who received cells generated in FCS-supplemented medium (Selvaggi et al., 1997), even leading to arrhythmias after cellular cardioplasty (Chachques et al., 2004). Serum-free medium or chemically defined medium containing growth factors needs to be developed for clinical trials (Lange et al., 2007). Fibroblast growth factor (FGF) is an important growth factor for expansion of mesenchymal stem cells. Basic FGF (bFGF) increases the growth rate of mesenchymal stem cells, and FGF signaling is essential for proliferation of mesenchymal stem cells (Ng et al., 2008). Platelet-derived growth factor (PDGF) signaling is also important in growth (Ng et al., 2008) and migration of mesenchymal stem cells, but not in differentiation. Furthermore, transforming growth factor- β (TGF- β) is important for proliferation of mesenchymal stem cells in a Smad-3 dependent manner.

In this study, we sought to determine whether a default-like mechanism underlies mesenchymal specification *in vitro* (Tropépe et al., 2001). We report here that chemically defined serum-free culture conditions are sufficient for maintenance of multipotent mesenchymal stem cells. Furthermore, proliferation of the mesenchymal stem cells can be enhanced by PDGF and/or bFGF-related signaling, in a manner that is consistent with a default model of mesenchymal fate specification.

Methods

Cells and cell culture

After signed informed consent was obtained, bone marrow cells, chondrocytes and preadipocytes were harvested from surgical specimens with the approval (approval number, #25 and #49) of the Ethics Committee of the National Institute for Child and Health Development, Tokyo. Cells were resuspended in Dulbecco's modified Eagle's medium (DMEM) and cultured as previously described (Imabayashi et al., 2003; Takeda et al., 2004; Mori et al., 2005). Several bone marrow stromal cell strains were generated from primary or first passage cells using the limiting dilution method. The dissected cartilage was digested for 30 min in 0.08% trypsin in Dulbecco's phosphate-buffered saline (PBS) at 37°C, followed by two washes with PBS. The cartilage was then digested by incubation with 0.1% collagenase for 1 h at 37°C in DMEM. The released chondrocytes were harvested by centrifugation. The harvested cells were plated onto culture dishes and cultured in LS (described below) medium or DMEM supplemented with 10% fetal calf serum. Adipose tissue was dissected and washed twice in PBS. The dissected tissue was plated onto culture dishes and cultured in DMEM supplemented with 10% fetal calf serum or LS growth medium. After several days, outgrowth of preadipocytes occurred. Adult human mesenchymal stem cells (Poietics normal Human Mesenchymal Stem Cells, catalog number: #PT-2501, lot number: 2F1657) were purchased from BioWhittaker (Walkersville, MD). We call these cells MF in this study to differentiate these cells from the general term 'mesenchymal cells' and avoid confusion. Mesenchymal stem cell growing medium (MSCGM) (BioWhittaker) was used for "conventional growth medium". α MEM basal medium supplemented with 1% FCS, insulin, transferrin, selenic acid, phosphoethanolamine, 10 ng/ml (0.31 nM) PDGF-BB, and 10 ng/ml (0.59 nM) bFGF was prepared as "low-serum (LS) growth

medium." H4-1, UE6E7T-12, UE7T-13 and H8-10 cells were cultured as previously described (Imabayashi et al., 2003; Takeda et al., 2004; Mori et al., 2005).

Flow cytometric analysis

Cells were detached and stained for 30 min at 4°C with primary antibodies and immunofluorescent secondary antibodies. After washing, the cells were analyzed using a CYTMETRIC FC500 flow cytometer (Beckman Coulter, Fullerton, CA). Antibodies to CD140a (aRI, BD Bioscience, San Jose, CA) and CD140b (28D4, BD Bioscience) were used as primary antibodies. As secondary antibodies, PE labeled Mouse IgG1 (Beckman Coulter) and IgG2a (PharMingen, San Diego, CA) were used.

Cell proliferation

Cell proliferative capacity was assessed by calculating the total number of population doublings (population doubling level or accumulative population doublings), using the formula $\log_{10}(\text{total number of cells}/\text{starting number of cells})/\log_{10} 2$. The number of cells was counted by ViCell (Beckman Coulter) at each passage. Cell proliferation was also measured by a colorimetric assay using 2-(4-iodophenyl)-3-(4-nitrophenyl)-5-(2,4-dissulfophenyl)-2H-tetrazolium (WST-1; Dojindo, Japan). Exponentially growing cells (3.5×10^3) were plated in a 24-well plate in 500 μ l per well of DMEM/20I combined medium supplemented with 5 μ g/ml insulin, 5 μ g/ml transferrin, and 0.5% serum. After 24 hr, the growth medium was changed to the medium containing growth factors. After incubation at 37°C for 4 days, 50 μ l of 3.2 mg/ml WST-1 was added to each well and incubated at 37°C for an additional 20 min. Optical densities were measured using a microplate reader with a wavelength of 450 nm.

Western blot analysis

To detect p16ink4a and tubulin, immunoblotting was performed as previously described (Sano et al., 2001) with antibodies against p16ink4a (G175-1239, BD Bioscience) and tubulin (TUB2.1, Sigma-Aldrich Japan, K.K., Tokyo, Japan).

GeneChip expression analysis

Human-genome-wide gene expression was examined with the Human Genome U133A Probe array (GeneChip, Affymetrix), which contains 22,283 oligonucleotide probe sets, according to the manufacturer's protocol (Expression Analysis Technical Manual and GeneChip small sample target labeling Assay Version 2 technical note. <http://www.affymetrix.com/support/technical/index.affx>).

Results

Effects of growth factors on growth of mesenchymal cells

To determine which growth factors are effective for promoting mesenchymal cell growth, we investigated the expression levels of growth factor receptors in H4-1, UE6E7T-12, and UE7T-13 cells by the DNA chip analysis (Table 1). All the cells tested expressed receptors for epidermal growth factor (EGF), platelet-derived growth factor (PDGF), insulin-like growth factor (IGF), transforming growth factor (TGF), and fibroblast growth factor (FGF). We therefore investigated the effects of VEGF, EGF, bFGF and PDGF on the growth of MF cells (Fig. 1A). Among the growth factors tested, PDGF and bFGF accelerated cell growth. After combination of the growth factors were tested, we decided to use PDGF and bFGF for subsequent experiments. To obtain maximum growth, we also examined the effects of basal medium, hormone, and fat precursors (data not shown). Based on the results, we established the low serum growth medium (LS medium: α MEM basal medium supplemented with 1% FCS, insulin, transferrin, selenic acid,